SAND2014-18722PE

Exceptional service in the national interest

Sandia National Laboratories

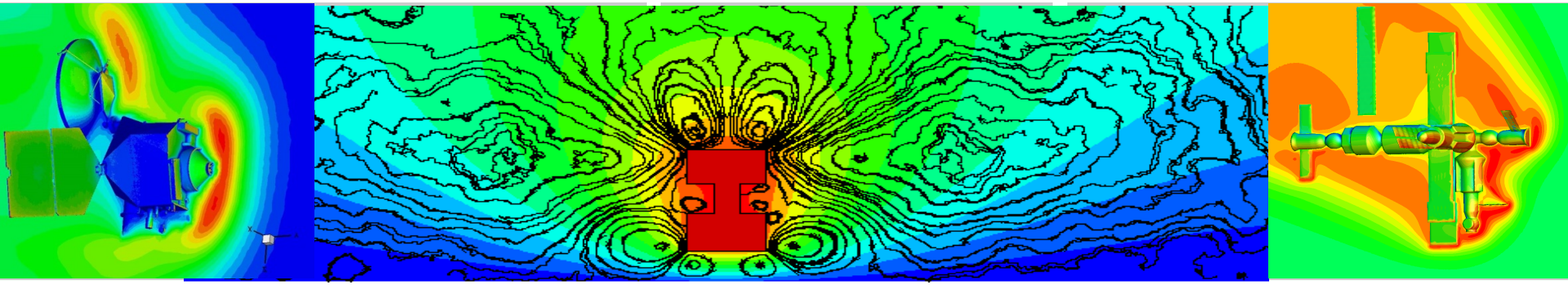

Towards Exascale Molecular Gas Dynamics Simulations

Michael A. Gallis

Engineering Sciences Center
Sandia National Laboratories
Albuquerque, New Mexico, USA

U.S. DEPARTMENT OF ENERGY

NNSA National Nuclear Security Administration

Sandia National Laboratories is a multi-program laboratory managed and operated by Sandia Corporation, a wholly owned subsidiary of Lockheed Martin Corporation, for the U.S. Department of Energy's National Nuclear Security Administration under contract DE-AC04-94AL85000.

The Space Shuttle Columbia Accident

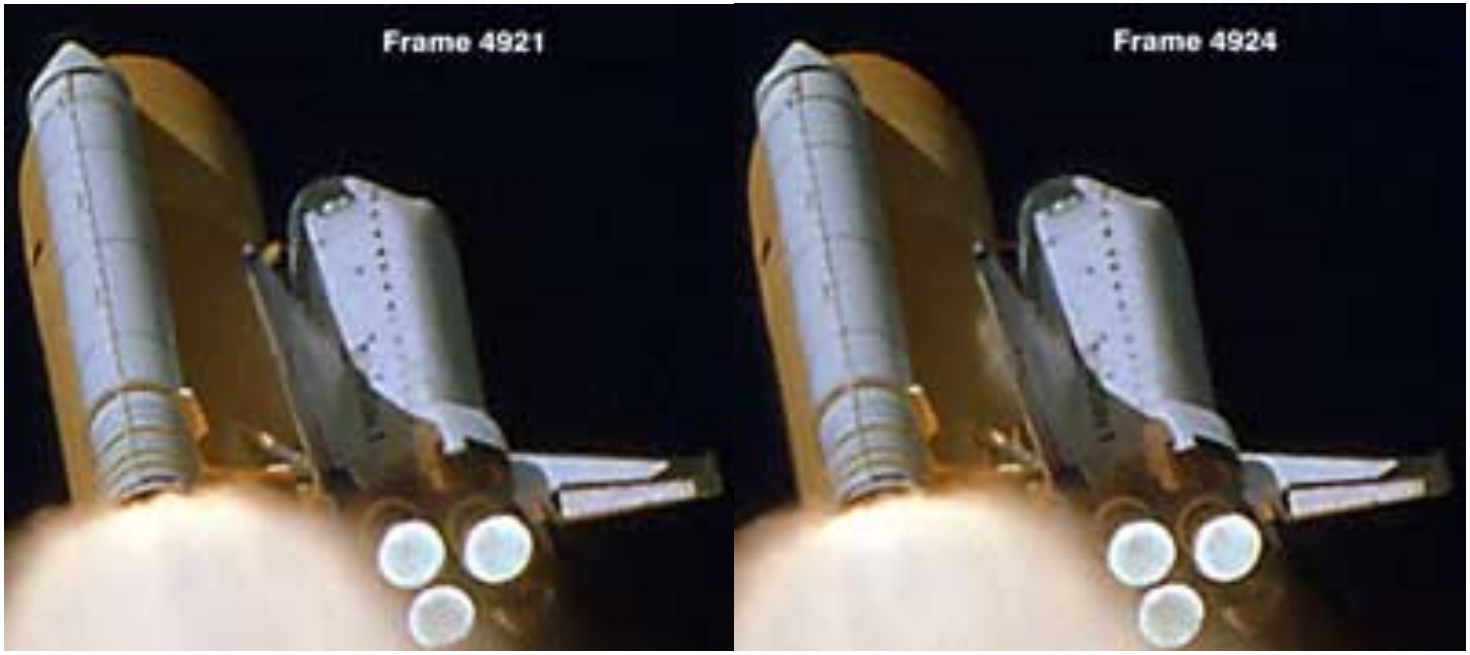

During the ascent phase a piece of insulating foam hit the leading edge of the left wing causing an approximately 10 inch hole.

Damage Scenario Investigated

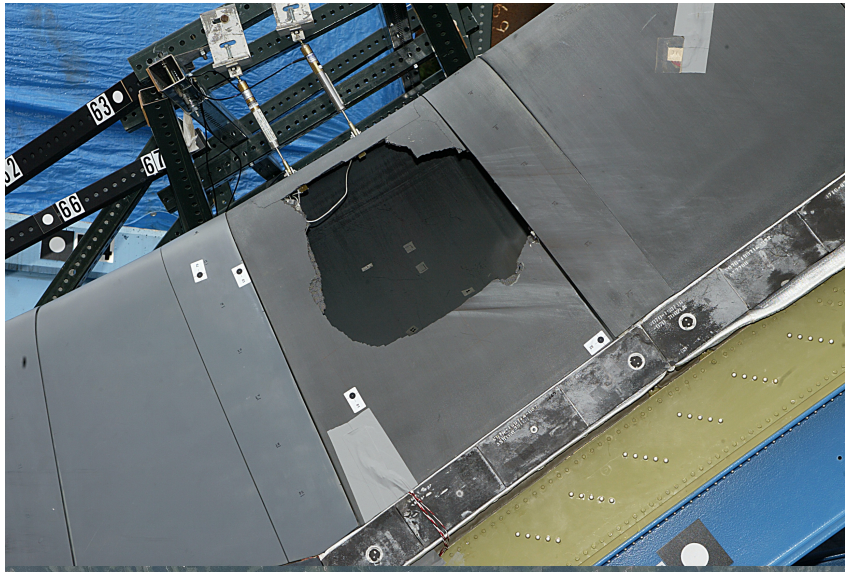

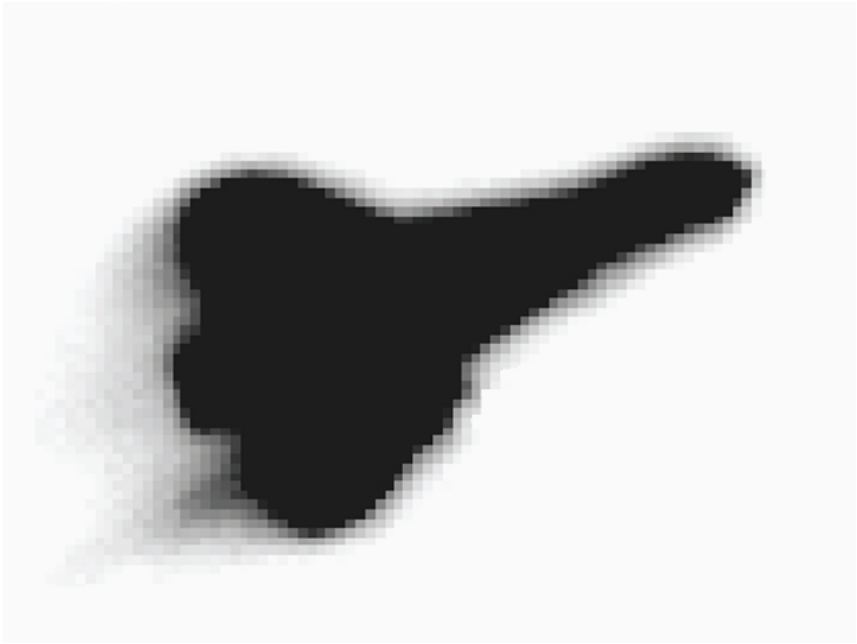

The resulting hole allowed overheated gases to penetrate the wing cavity, compromise its structural integrity, leading to a loss of the vehicle during descent

Numerical Simulations Supporting the Investigation

Sandia National Laboratories

Simulation conditions

Altitude = 350,000-300,000 ft

Mach Number = 27

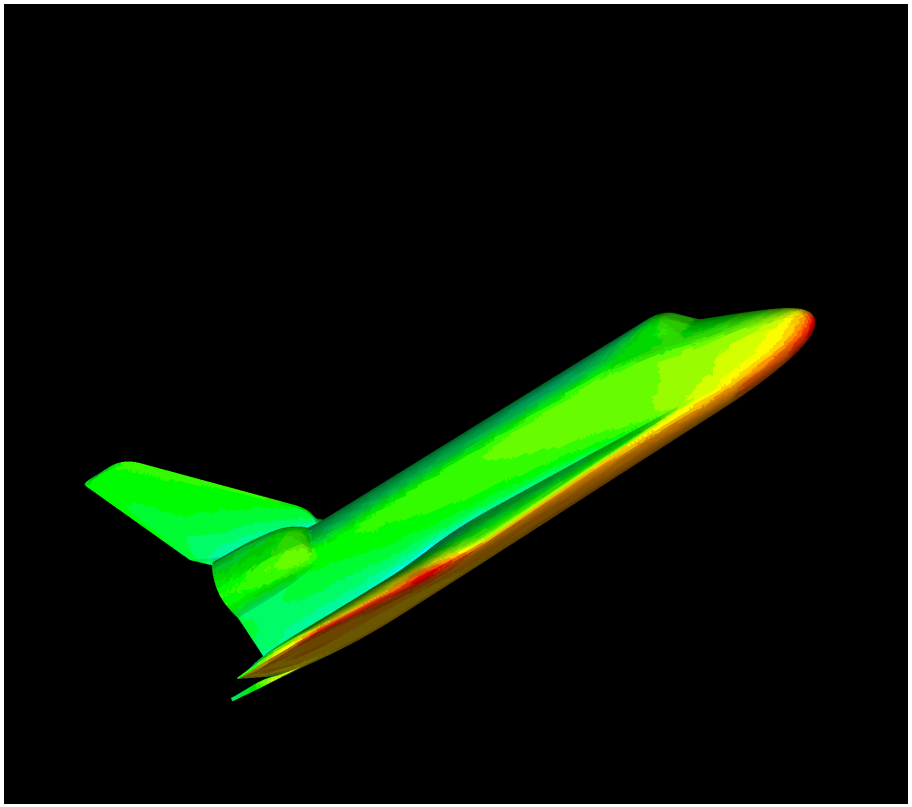

Temperature and Heating Profile

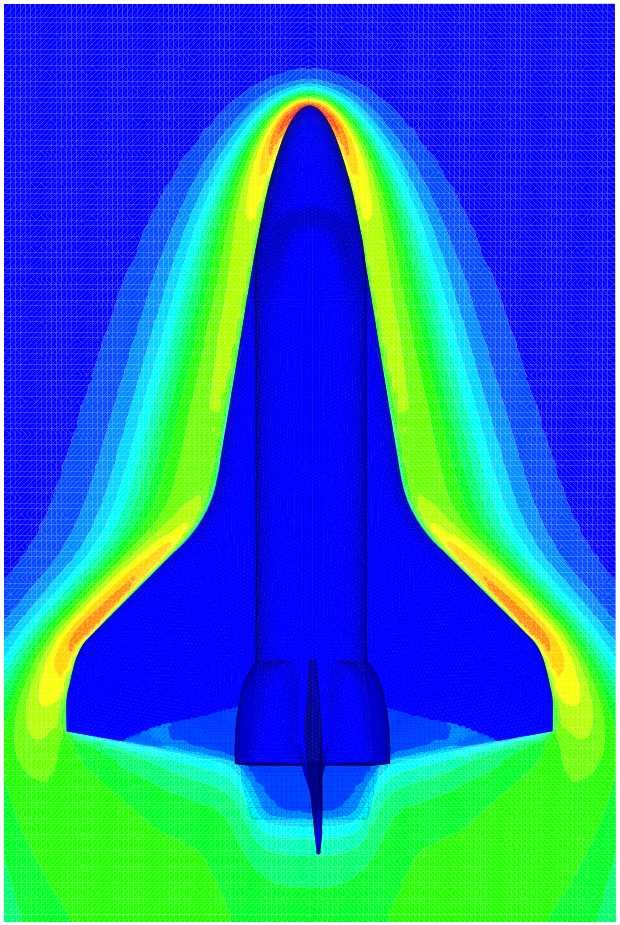

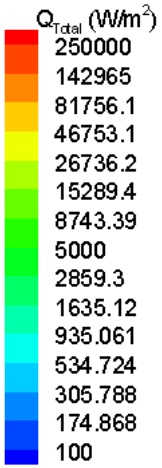

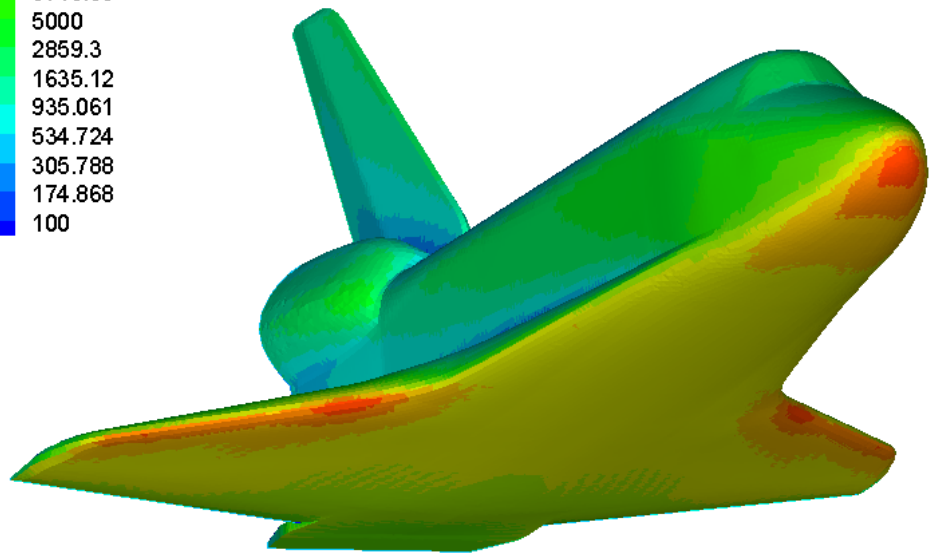

Flow Inside the Wing Cavity

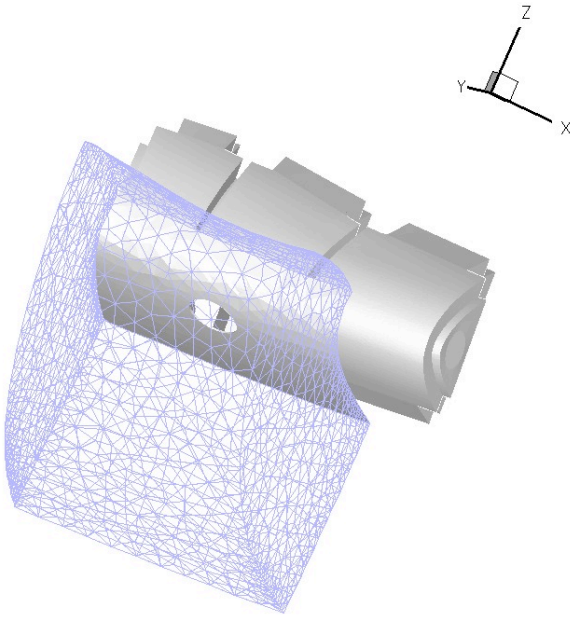

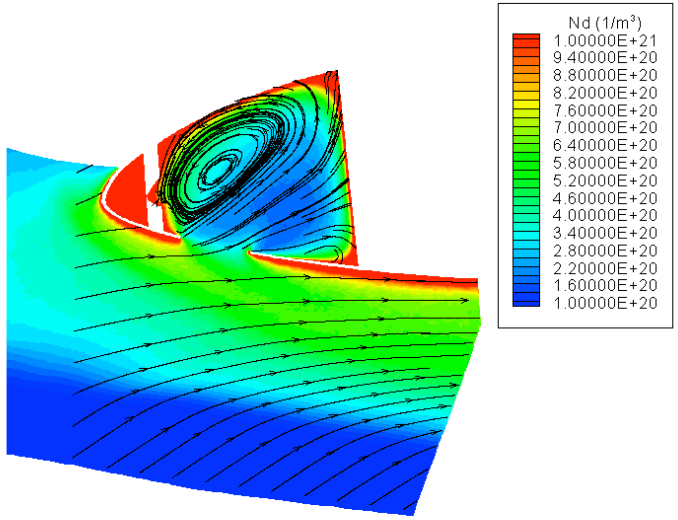

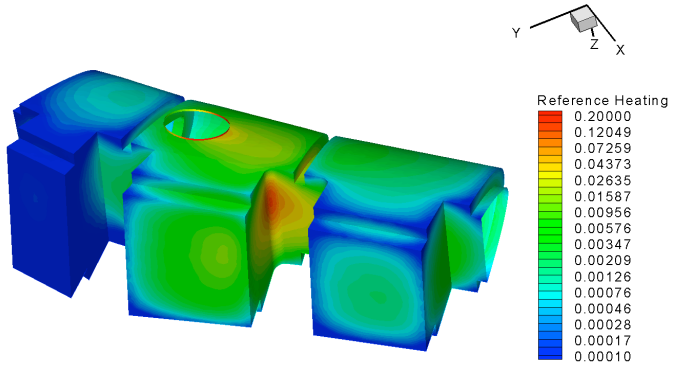

The Non-continuum/Non-equilibrium Regime

High Mach number flight is more easily achieved in rarefied conditions (non-continuum).

Non-continuum conditions prevail, leading to flows out of thermodynamic equilibrium.

This flight regime results in high temperatures (more than 10,000K), chemically reacting, ionizing flows.

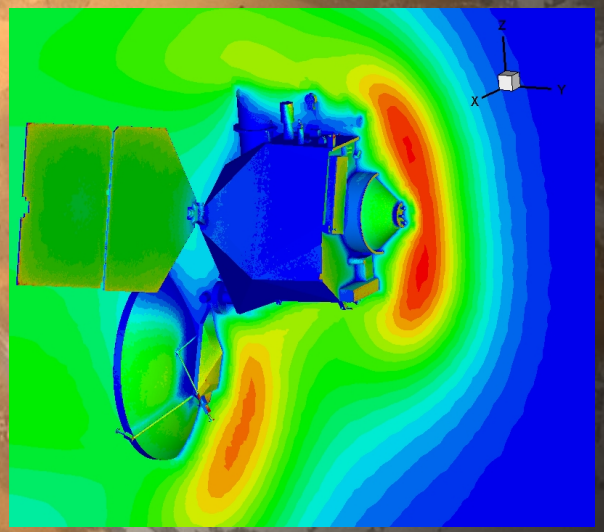

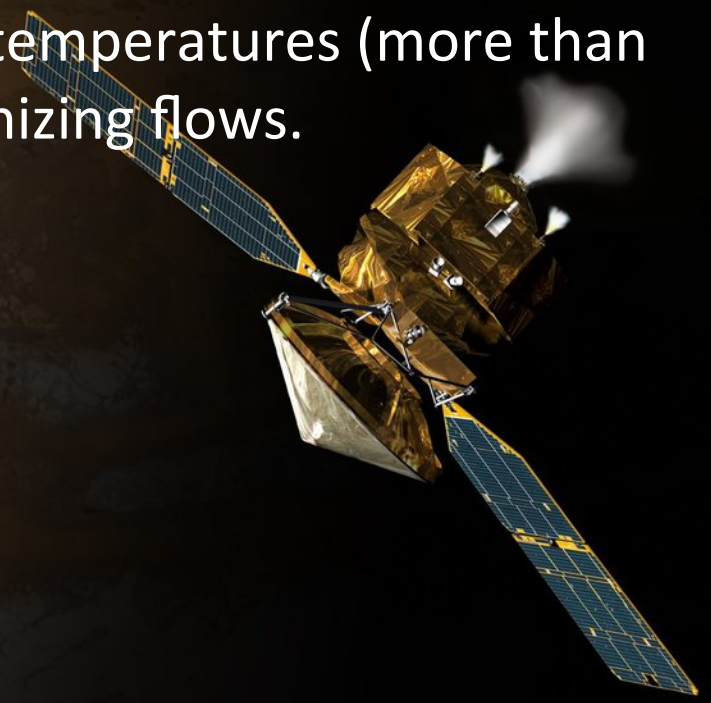

The Non-continuum/Non-equilibrium Regime

Sandia National Laboratories

High Mach number flight is more easily achieved in rarefied conditions (non-continuum).

Non-continuum conditions prevail, leading to flows out of thermodynamic equilibrium.

This flight regime results in high temperatures (more than 10,000K), chemically reacting, ionizing flows.

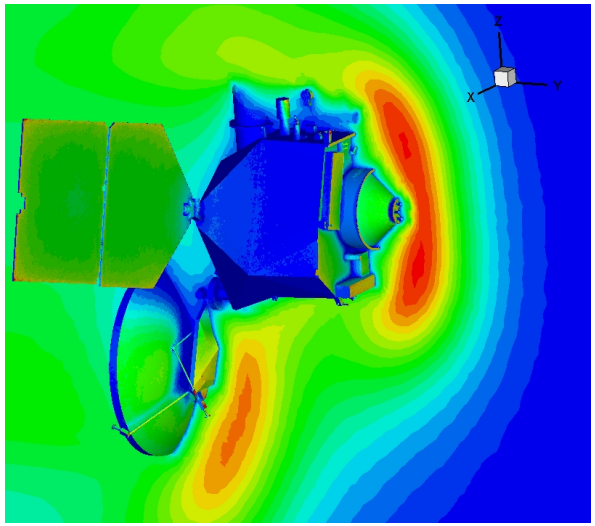

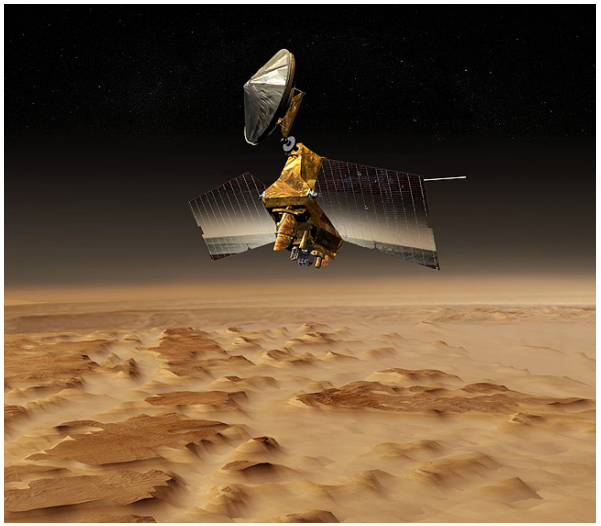

Continuum but Non-equilibrium in MEMS Heated Microbeam Near Substrate

Sandia National Laboratories

Micro Electro Mechanical Systems (MEMS) reawakened interest in gas flow through long thin channels/tubes

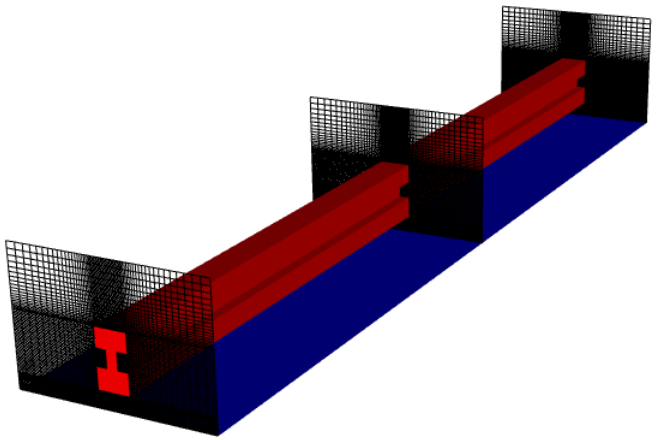

Solid regions: silicon

- Geometry: 2-micron gap
- Beam temperature: ~900 K
- Substrate temperature: ~300 K

Gas region: nitrogen

- Pressure: atmospheric
- Initial temperature: ~300 K

Heated Microbeam makes Gas Move

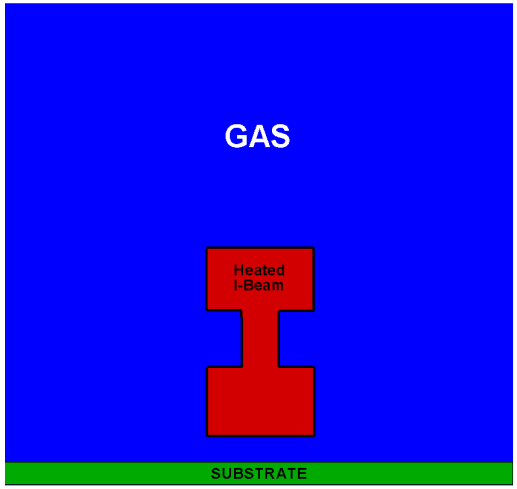

DSMC microbeam simulations

- Steady gas motion is induced by temperature differences

  Not buoyancy, *not* transient
- Noncontinuum effects cause motion

  Not seen in NSSJ simulations

1 atm
~0.1 m/s

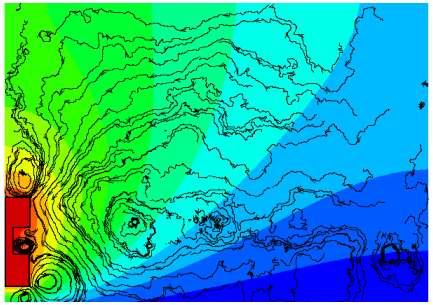

0.1 atm
~2 m/s

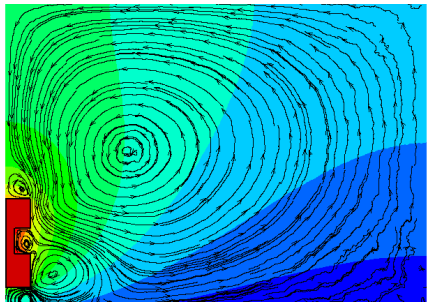

0.01 atm
~1 m/s

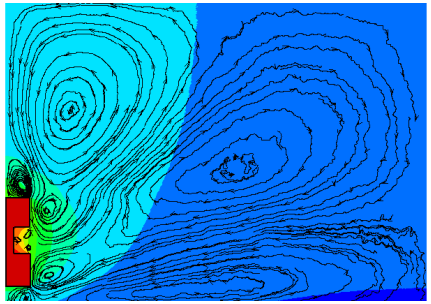

Length Scales for Dilute Gases

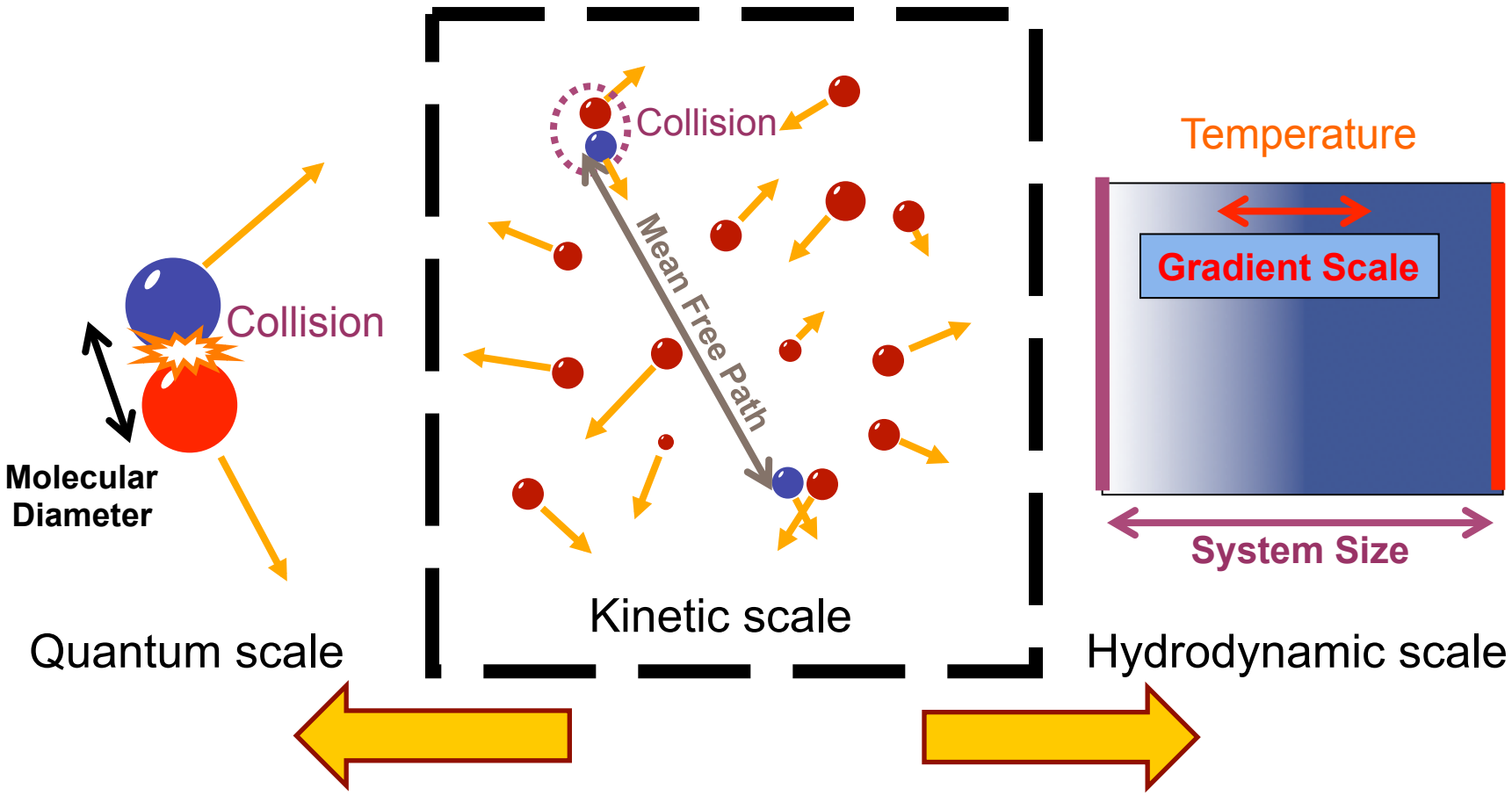

Simulating the Kinetic Regime

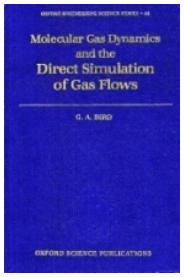

- "In general, the field or rarefied gas flow problems is still largely unclarified" last sentence from *Elements of Gasdynamics (1956)* by H. W. Liepmann and A. Roshko.
- The Direct Simulation Monte Calro (DSMC) originated in 1963* by Graeme A. Bird, encouraged by H. Liepmann.

  * "G. A. Bird, 'Approach to translational equilibrium in a rigid sphere gas', Phys. Fluids, 6, p1518 (1963)".
- The objective of DSMC is to simulate complicated gas flows using only collision mechanics of simulated molecules
- Today, DSMC is the dominant numerical algorithm at the kinetic scale
- DSMC applications are expanding to multi-scale problems creating new challenges and opportunities.

Direct Simulation Monte Carlo

Sandia National Laboratories

How DSMC works

- Computational molecules move ballistically, collide statistically, and interact statistically with surfaces like real molecules
- Molecular movement, surface-interaction, and collision are implemented sequentially in the algorithm
- Cell-based molecular statistics (“moments”) are sampled and averaged over many time steps for steady flow

DSMC issues

- Statistical aspect requires $O(10^9)$ samples for flows (~1 m/s)

DSMC is inherently a transient method

- Steady state is the ensemble average of unsteady state moves

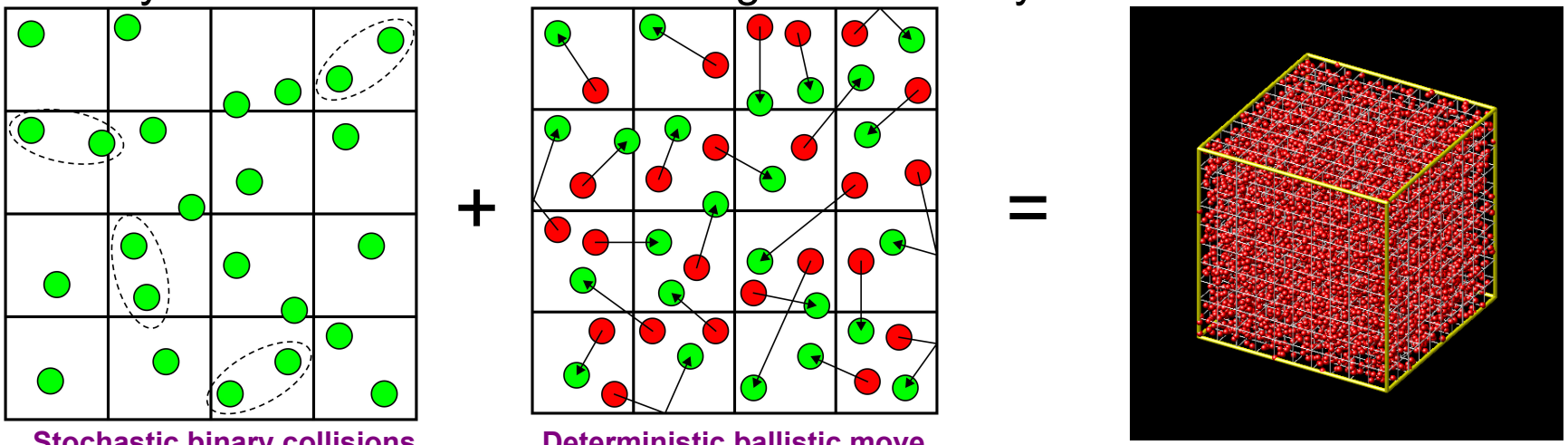

Stochastic binary collisions

Deterministic ballistic move

Boltzmann Equation and the Direct Simulation Monte Carlo Method

Sandia National Laboratories

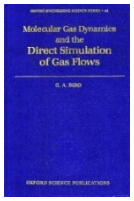

Graeme Bird (1963, 1994)

molecules move **molecules collide**

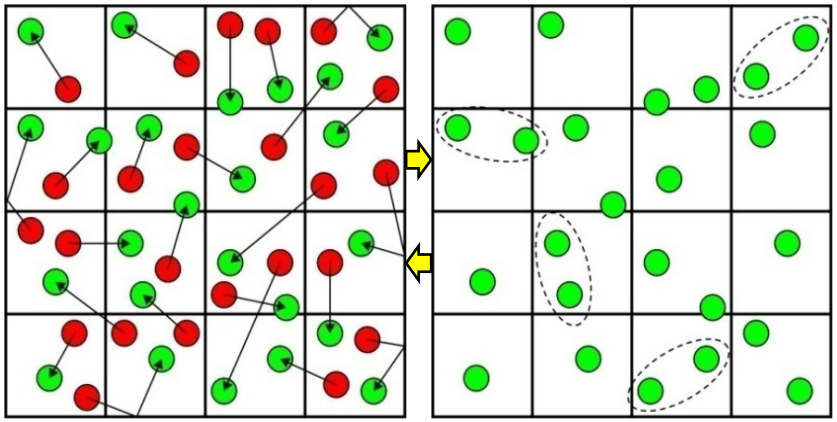

Ludwig Boltzmann

$$\frac{\partial f}{\partial t} + \mathbf{v}\cdot\frac{\partial f}{\partial \mathbf{x}} + \frac{\mathbf{F}}{m}\cdot\frac{\partial f}{\partial \mathbf{v}} = \int_{-\infty}^{\infty}\int_{0}^{4\pi}\left(f^{*}f_{1}^{*} - ff_{1}\right)\left|\mathbf{v}-\mathbf{v}_{1}\right|\sigma\, d\Omega\, d\mathbf{v}_{1}$$

molecular motion and force-induced acceleration

pairwise molecular collisions (molecular chaos)

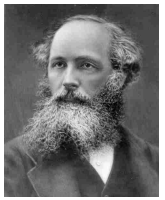

James Clerk Maxwell

DSMC vs. Boltzmann Equation

Sandia National Laboratories

- Instead of solving Newton's laws of motion (Molecular Dynamics), DSMC replaces explicit intermolecular forces with stochastic collisions
- It has been shown that DSMC is equivalent to solving the Boltzmann equation (Nambu 1980, Babovsky 1989, Wagner 1992)
- DSMC has been shown to reproduce exact known solutions (Chapman-Enskog, Moment Hierarchy) of the Boltzmann equation (Gallis et al. 2004, 2006) for non-equilibrium flows
- In fact, DSMC is superior to solving the Boltzmann equation
  - DSMC can model complicated processes (e.g., polyatomic molecules, chemically reacting flows, ionized flows) for which Boltzmann-type transport equations are not even known (Struchtrup 2005)
  - DSMC includes fluctuations, which have been shown to be physically realistic (Garcia 1990) but which are absent from the Boltzmann equation

The objective of DSMC is to simulate complicated gas flows using only collision mechanics of simulated molecules in the regime described by the Boltzmann equation

Chapman-Enskog (CE) Theory

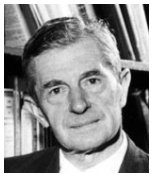

Sydney Chapman

David Enskog

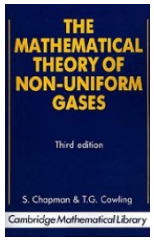

$$f = f^{(0)}(1+\Phi^{(1)}+\Psi^{(1)}) \qquad f^{(0)} = (n/\pi^{3/2}c_m^3)\exp[-\tilde{c}^2]$$

$$c_m = \sqrt{2k_BT/m} \qquad \tilde{\mathbf{c}} = \mathbf{c}/c_m \quad \mathbf{c} = \mathbf{v}-\mathbf{u}$$

$$\Phi^{(1)} = -(8/5)\tilde{A}[\tilde{c}]\tilde{\mathbf{c}}\cdot\tilde{\mathbf{q}} \qquad \Psi^{(1)} = -2\tilde{B}[\tilde{c}](\tilde{\mathbf{c}}\circ\tilde{\mathbf{c}}:\tilde{\tau})$$

$$K = -(5/4)k_Bc_m^2a_1 \qquad \mu = (1/2)mc_m^2b_1$$

$$\tilde{A}[\tilde{c}] = \sum_{k=1}^{\infty}(a_k/a_1)S_{3/2}^{(k)}[\tilde{c}^2] \qquad \tilde{B}[\tilde{c}] = \sum_{k=1}^{\infty}(b_k/b_1)S_{5/2}^{(k-1)}[\tilde{c}^2]$$

$$C_p = (5/2)(k_B/m) \qquad \mathrm{Pr} = (2/3)(\mu_\infty/\mu_1)(K_1/K_\infty)$$

- Chapman and Enskog analyzed Boltzmann collision term
  - Perturbation expansion using Sonine polynomials
  - Near equilibrium, appropriate in continuum limit
- Determined velocity distribution and transport properties
  - Thermal conductivity K, viscosity m, mass self-diffusivity D
  - Prandtl number Pr from "infinite-to-first" ratios K_∞/K_1, m_∞/m_1
  - Distribution "shape": Sonine polynomial coeffs. a_k/a_1, b_k/b_1
  - Values for all Inverse-Power-Law (IPL) interactions
    - Maxwell and hard-sphere are special cases

Extracting CE Parameters from DSMC

Sandia National Laboratories

$$q = K_{eff}\left(\frac{\partial T}{\partial x}\right) \qquad \frac{a_k}{a_1} = \sum_{i=1}^{k}\left(\frac{(-1)^{i-1}k!(5/2)!}{(k-i)!i!(i+(3/2))!}\right)\left(\frac{\left\langle \tilde{c}^{2i}\tilde{c}_x\right\rangle}{\left\langle \tilde{c}^{2}\tilde{c}_x\right\rangle}\right) \qquad \tilde{\mathbf{c}} = \frac{\mathbf{v}-\mathbf{V}}{c_m}$$

$$\tau = \mu_{eff}\left(\frac{\partial V}{\partial x}\right) \qquad \frac{b_k}{b_1} = \sum_{i=1}^{k}\left(\frac{(-1)^{i-1}(k-1)!(5/2)!}{(k-i)!(i-1)!(i+(3/2))!}\right)\left(\frac{\left\langle \tilde{c}^{2(i-1)}\tilde{c}_x\tilde{c}_y\right\rangle}{\left\langle \tilde{c}_x\tilde{c}_y\right\rangle}\right) \qquad c_m = \sqrt{\frac{2k_BT}{m}}$$

DSMC moments of velocity distribution function

- Temperature T, velocity V
- Heat flux q, shear stress t
- Higher-order moments

DSMC values for VSS molecules (variable-soft-sphere)

- Thermal conductivity and viscosity: K_{eff} and m_{eff}
- Sonine-polynomial coefficients: a_k/a_1 and b_k/b_1
- Applicable for arbitrary Kn_L, Kn_q, Kn_t

Fourier and Couette Flow

Joseph Fourier

$$q = -K\frac{\partial T}{\partial x}$$

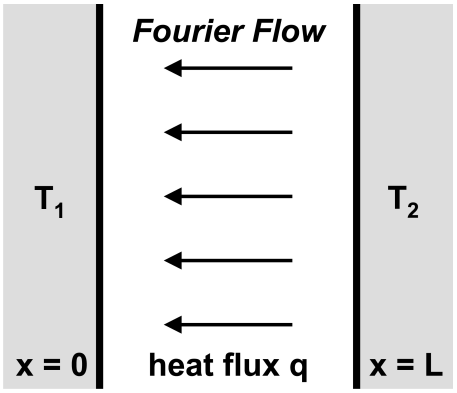

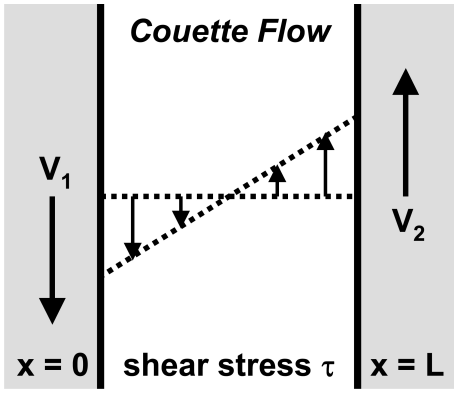

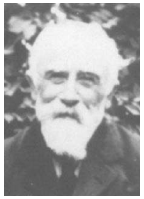

Maurice Couette

$$\tau = \mu\frac{\partial v}{\partial x}$$

Investigate transport in gas between parallel plates

- Fourier flow: heat conduction in stationary gas
- Couette flow: momentum transport in isothermal shear flow

Apply DSMC to Fourier flow and Couette flow

- Heat flux, shear stress: one-dimensional, steady

Compare DSMC to analytical "normal solutions"

- Normal: outside Knudsen layers
- Solutions: Chapman-Enskog (CE), Moment-Hierarchy (MH)

Verify DSMC accuracy at arbitrary heat flux, shear stress

- Thermal conductivity, viscosity; velocity distribution

Temperature and Velocity Profiles

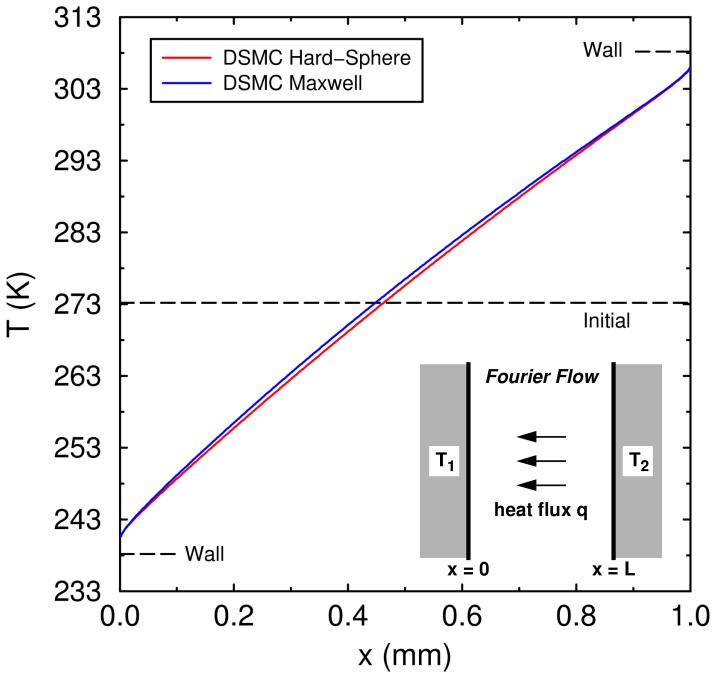

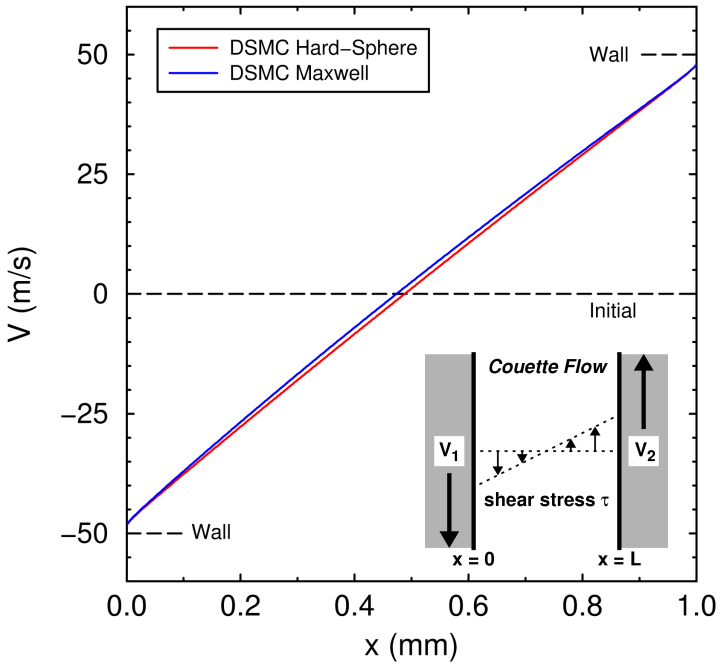

Low heat flux and shear stress: $Kn_q = 0.006$, $Kn_t = 0.003$

- Argon-like: initial T = 273.15 K, p = 266.644 Pa, l = 24 mm
- Walls: L = 1 mm = 42l, DT = 70 K, DV = 100 m/s
- $N_c = 120$, Dt = 7 ns, Dx = 2.5 mm, ~10^9 samples/cell, 32 runs

Small velocity slips, temperature jumps, Knudsen layers

DSMC Reproduces Infinite-Approximation Chapman-Enskog Transport Coefficients

Sandia National Laboratories

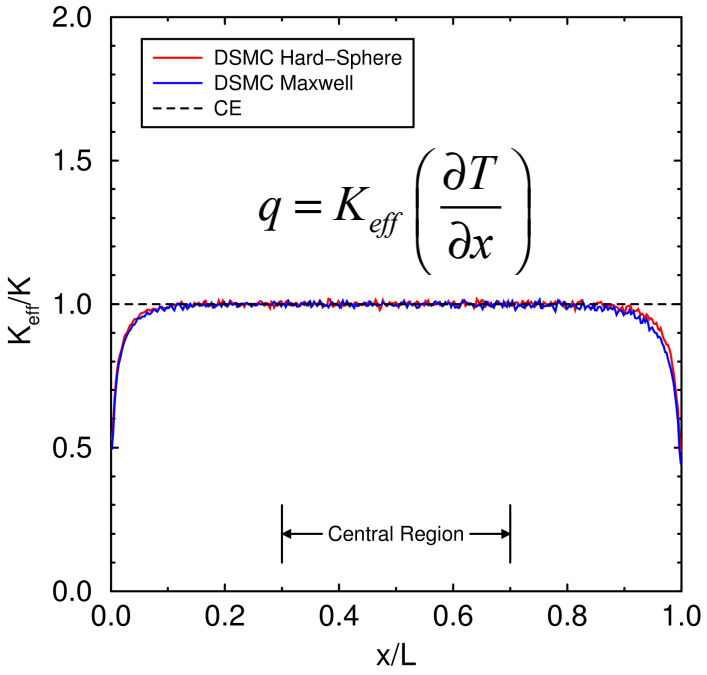

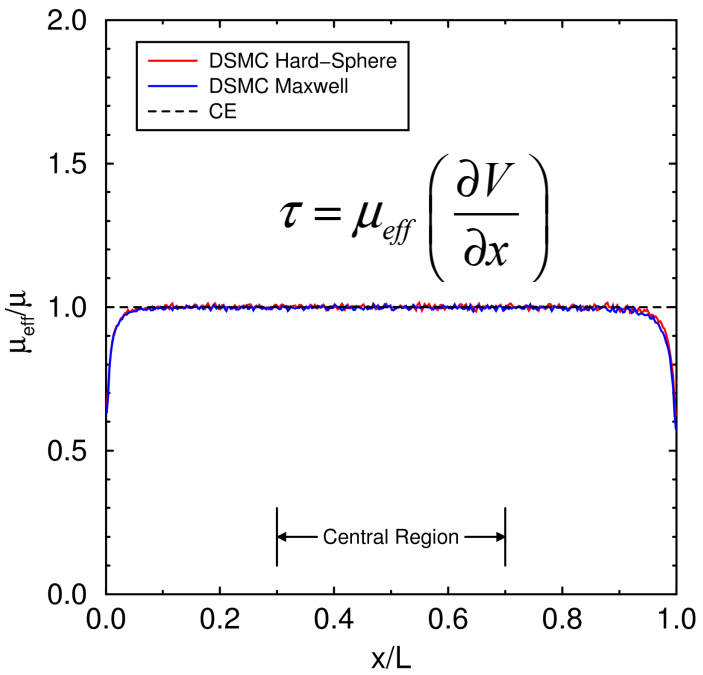

Thermal conductivity (left) and viscosity (right) away from walls

- Maxwell and hard-sphere results bound most gases
- Agreement with Chapman-Enskog theory verifies DSMC

DSMC Reproduces Infinite-Approximation Chapman-Enskog Velocity Distribution

Sandia National Laboratories

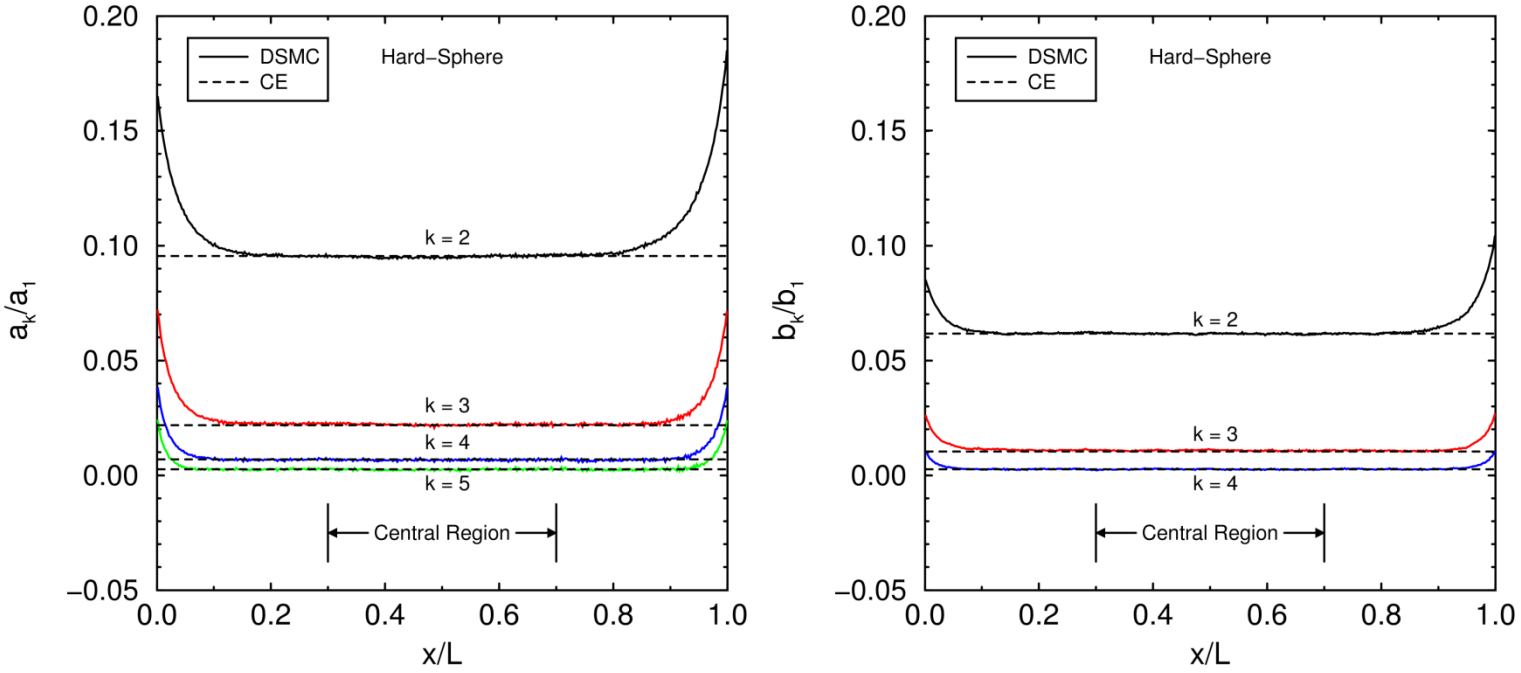

Sonine polynomial coefficients for temperature (left) & velocity (right) gradients

- **Hard-sphere values are shown, other interactions have similar agreement**
- **Higher-order (k > 5) coefficients (not shown) also have similar agreement**

Gallis M. A., Torczynski J. R., Rader D. J., "Molecular Gas Dynamics Observations of Chapman-Enskog Behavior and Departures Therefrom in Nonequilibrium Gases", *Physical Review E*, 69, 042201, 2004.

Maxwell Sonine-Coefficient Profiles

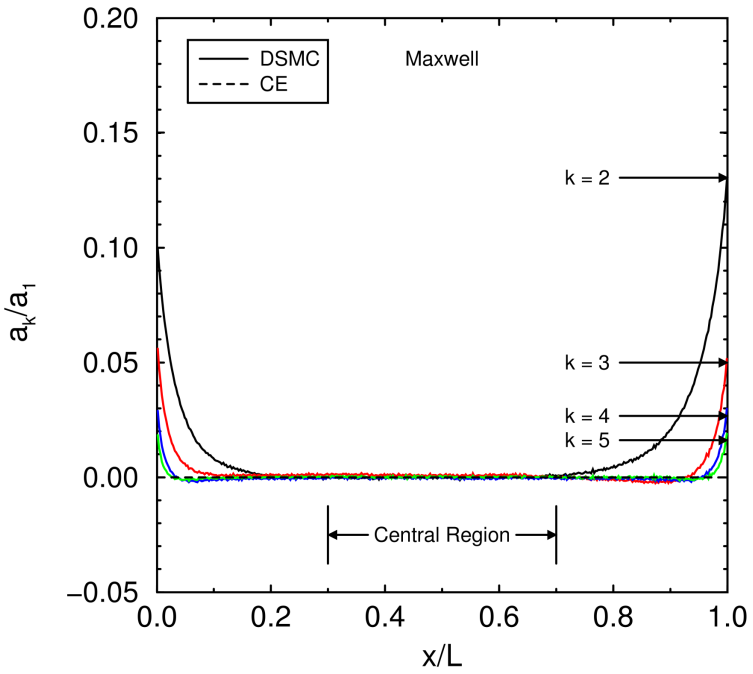

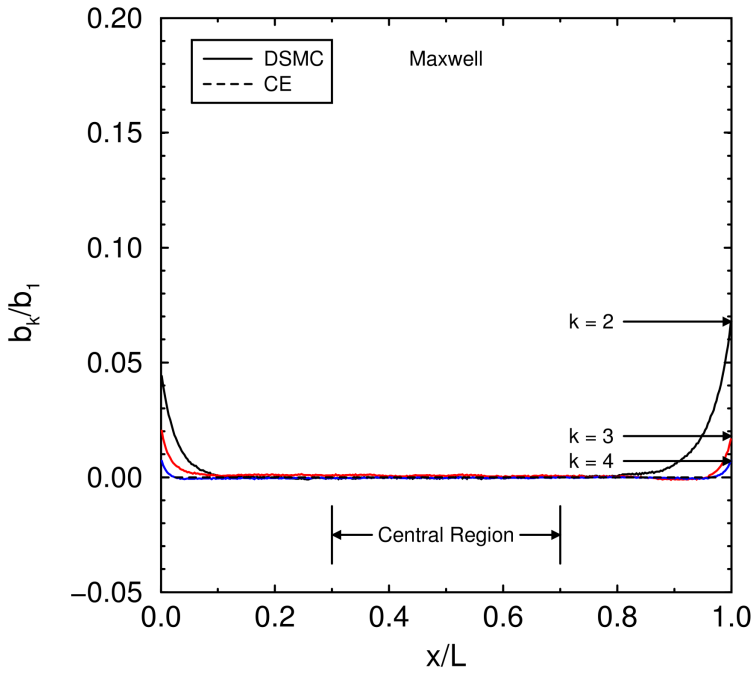

DSMC and CE Maxwell coefficients a_k/a_1 and b_k/b_1

- Low heat flux, low shear stress: $Kn_q = 0.006$, $Kn_t = 0.003$
- Good agreement in central region: normal solution
- Knudsen layers easily observed: ~10% of domain

Moment-Hierarchy Method

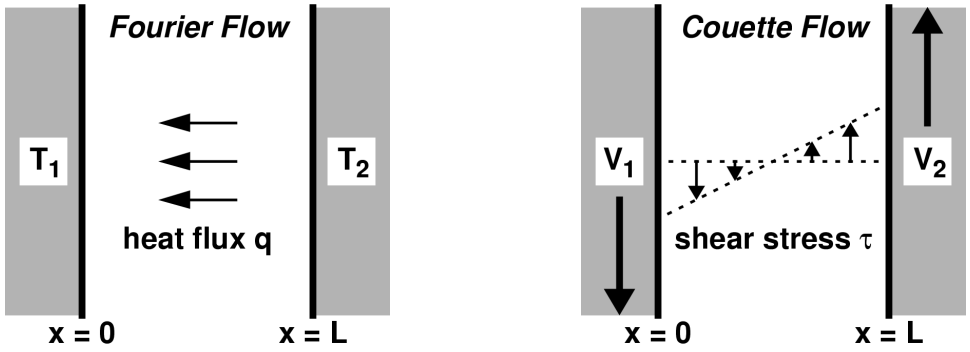

Moment-Hierarchy (MH) normal solution

- Santos and co-workers: theory, computer algebra
- Maxwell molecules: collision term quadratic in moments
- MH solution extends CE solution to finite Kn_q and Kn_t

Compare DSMC to MH for Maxwell molecules

- Dependence of Sonine coefficients on Kn_q known
- Thermal conductivity and viscosity independent of Kn_q
- Thermal conductivity and viscosity decrease with Kn_t

Apply DSMC for Maxwell molecules

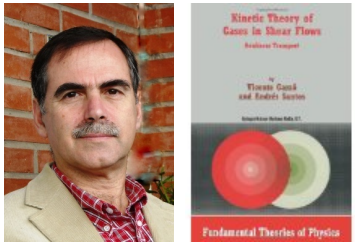

Andres Santos

Gallis M. A., Torczynski J. R., Rader D. J., Tij M., Santos A., "Normal Solutions of the Boltzmann Equation for Highly Nonequilibrium Fourier and Couette Flow", *Phys. Fluids, 18, 017104,* 2006.

Maxwell Normalized Sonine Coefficients

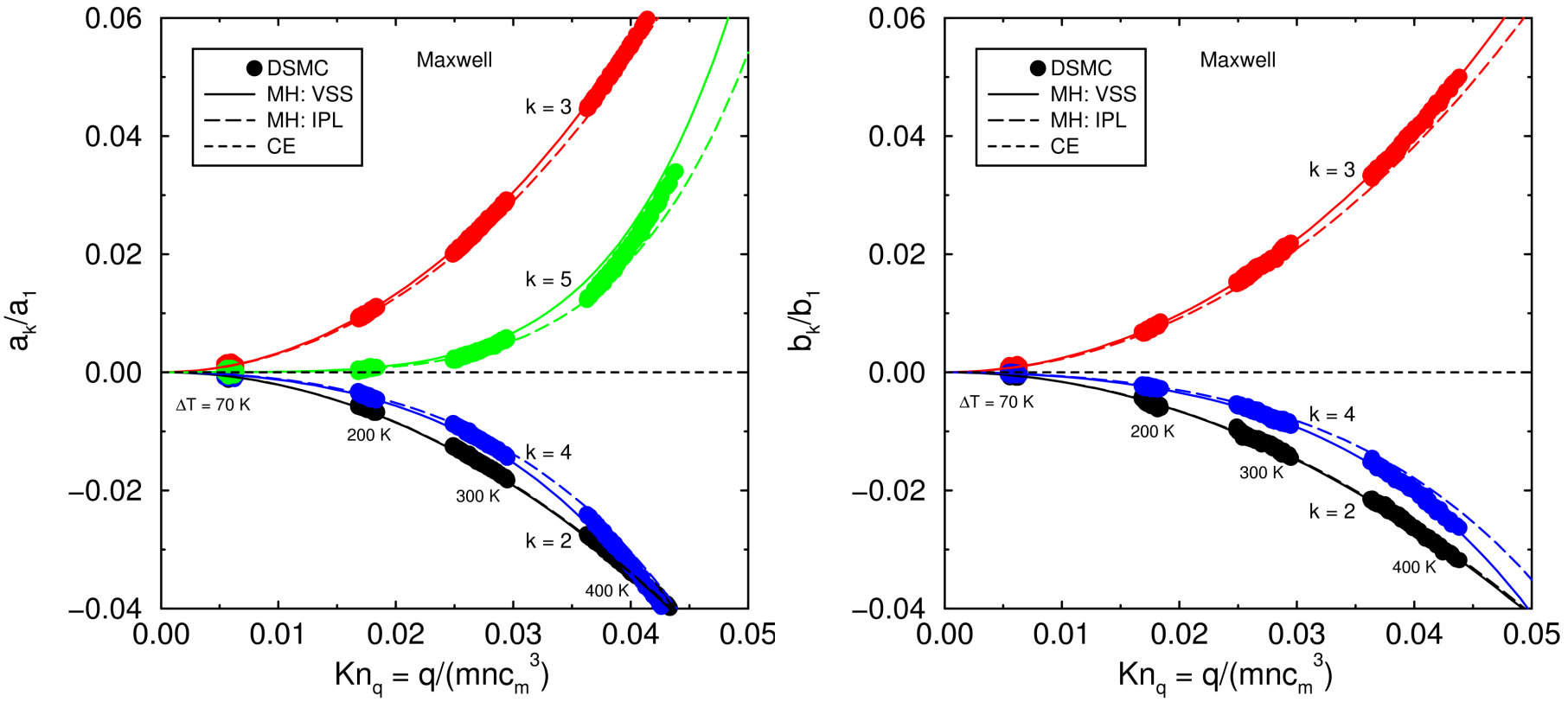

DSMC and MH Maxwell normal solutions for a_k/a_1 and b_k/b_1

- Four DSMC simulations: DT = 70, 200, 300, 400 K
- MH: VSS-Maxwell (solid) and IPL-Maxwell (dashed) differ
- DSMC and MH VSS-Maxwell normal solutions agree

Maxwell Normal Transport Coefficients

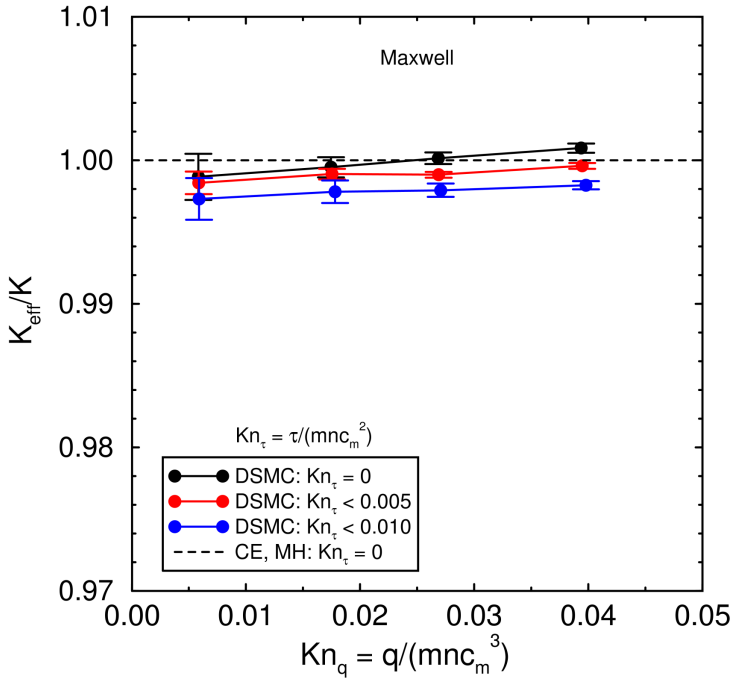

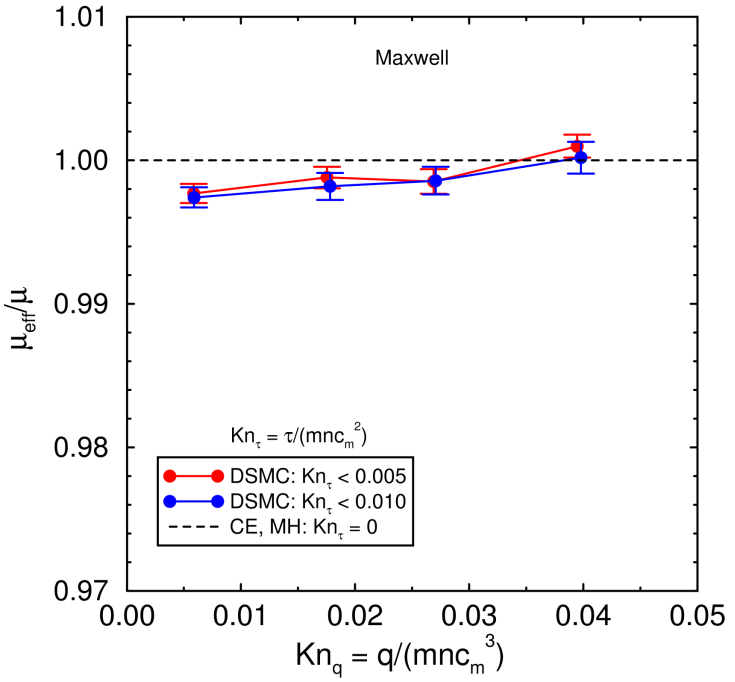

DSMC and MH Maxwell normal solutions for K and m

- DSMC profiles look like low-Kn_q profiles
- MH values for $Kn_t = 0$ are independent of Kn_q
- DSMC values approach MH values as $Kn_t \rightarrow 0$
- DSMC values increase very slightly with Kn_q

Agree to within DSMC discretization error

Hard-Sphere Normal Transport Coefficients

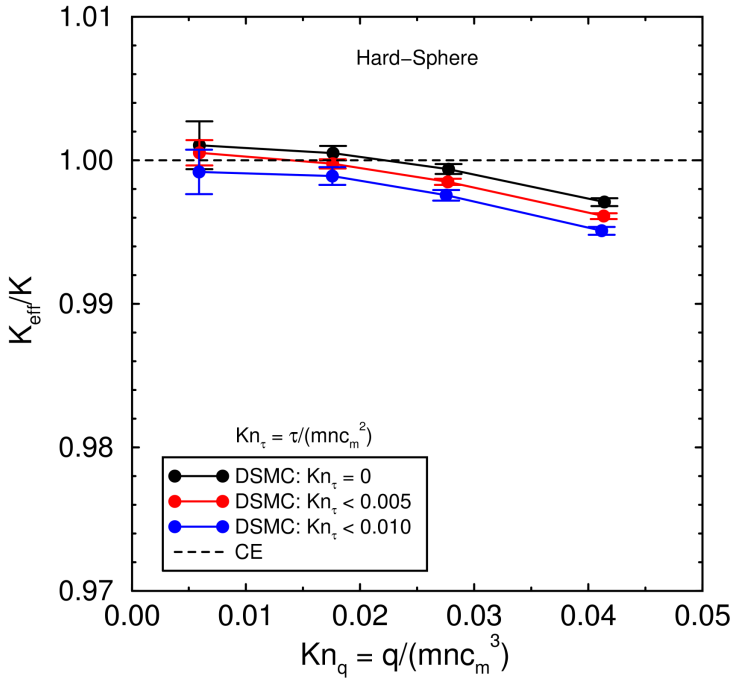

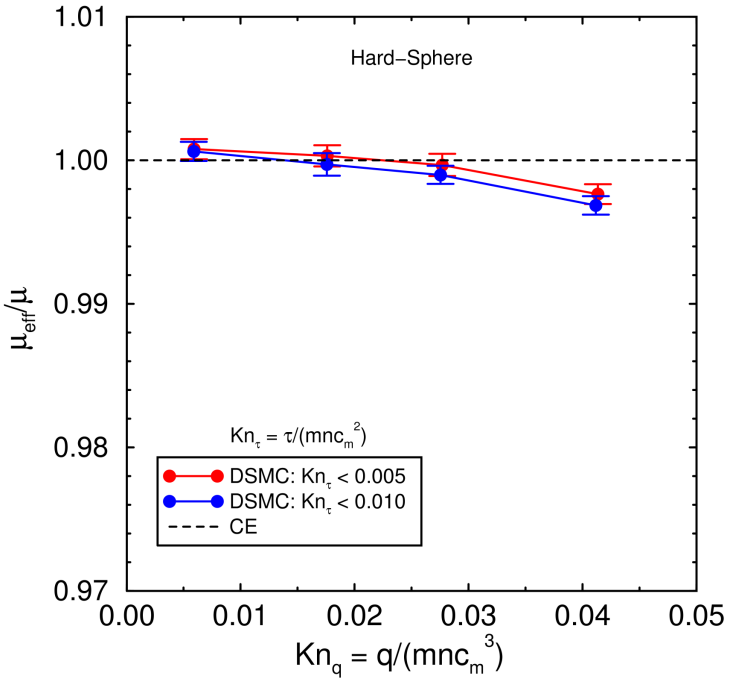

DSMC hard-sphere normal solution for K and m

- No theoretical results available: MH does not apply
- DSMC values decrease slightly with Kn_q
- Difference apparently greater than discretization error

Hard-sphere gas: “flux-insulating” and “flux-thinning”

Maxwell Normal Transport Coefficients

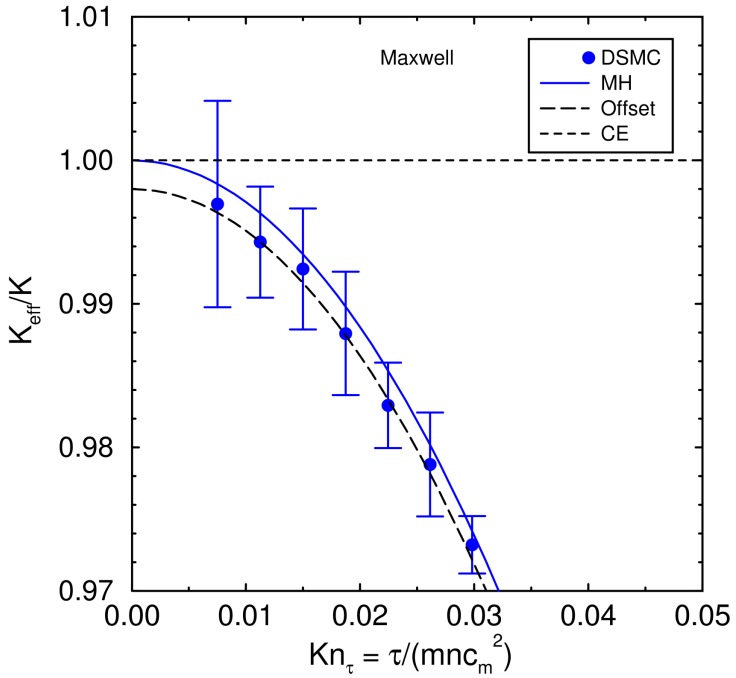

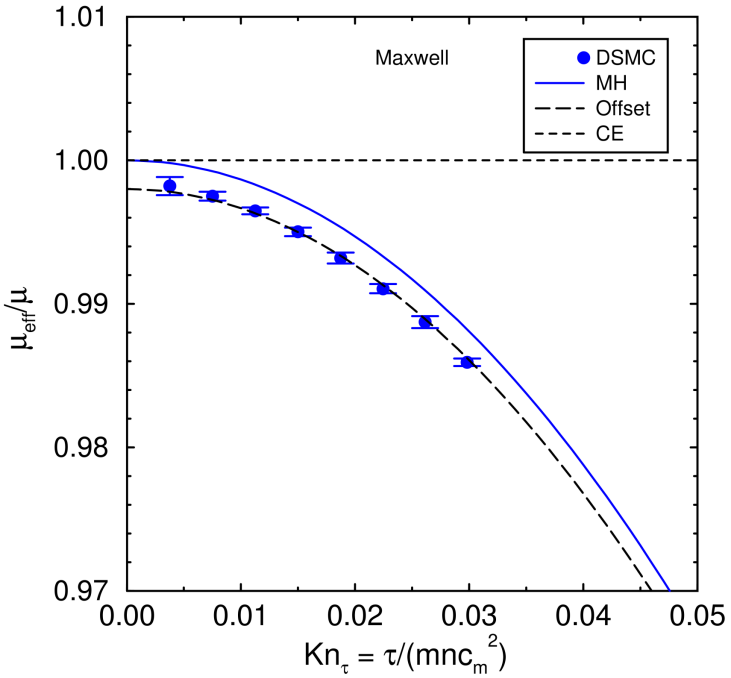

DSMC and MH Maxwell normal solutions for K and m

- Finite Kn_t (shear stress), low Kn_q (heat flux)
- Eight DSMC simulations: DV = 100, …, 800 m/s
- Thermal conductivity from viscous heating, larger errors
- Offset MH by DSMC discretization error

Agree to within DSMC discretization error

Hard-Sphere Normal Transport Coefficients

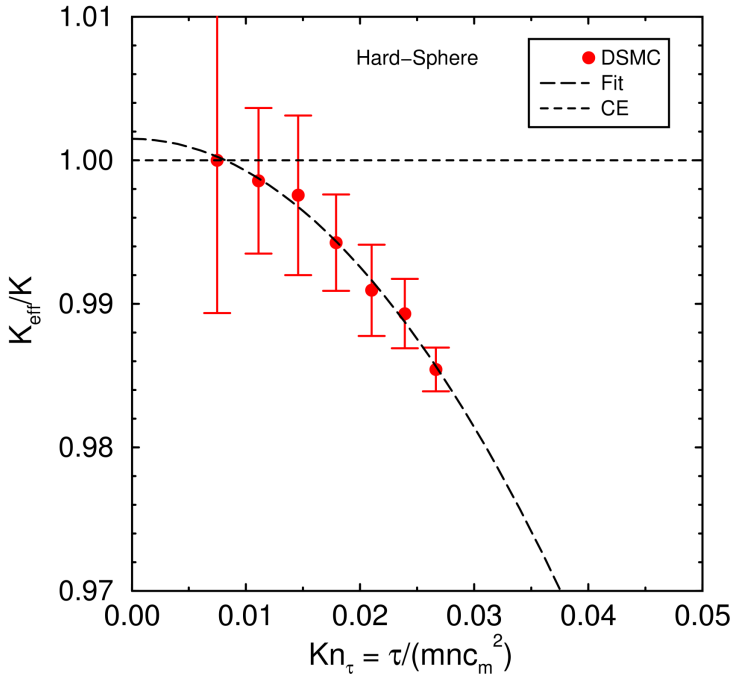

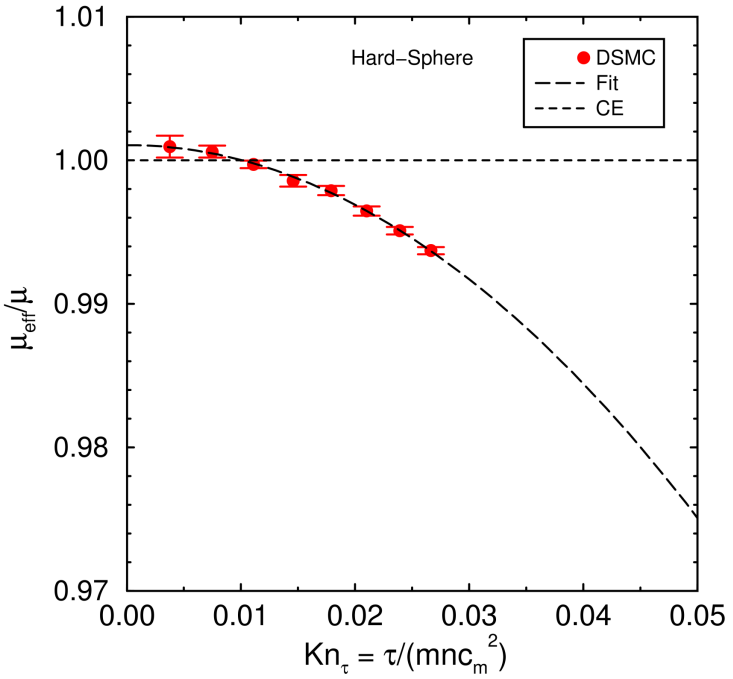

DSMC hard-sphere normal solution for K and m

- Finite Kn_t (shear stress), low Kn_q (heat flux)
- No theoretical results available: MH does not apply
- DSMC values decrease with Kn_t (like Maxwell)

Hard-sphere gas: “shear-insulating” and “shear-thinning”

DSMC Numerical Error

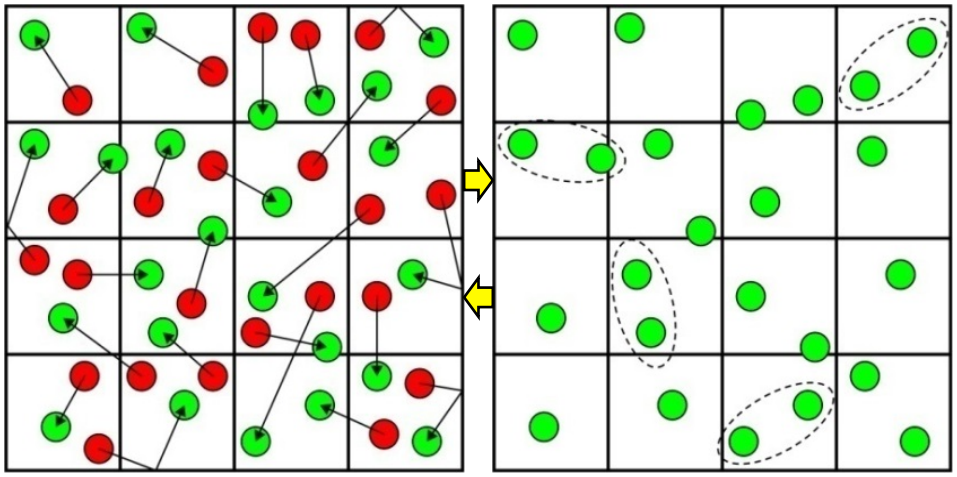

molecules move molecules collide

Four parameters control DSMC error:

Statistical error (1)

Samples per cell (S_c)

Discretization error (3)

- Particles per cell (N_c)
- Cell size (Δx)
- Time step (Δt)

Statistical and Particle-Number Errors

Sandia National Laboratories

Error related to sample size

- Statistical error
- Cell sample size $S_c = N_c \times N_t$
- N_c = particles per cell; N_t = time steps

Strategies for overcoming statistical error

- Use large number of samples
- For steady flows, use time and/or ensemble averaging
- Computational expense ~ S_c

Error related to local number of particles

- Error $\sim 1/N_c$
- Systematic – persists even as $S_c \rightarrow \infty$

Limited number of samples per time step

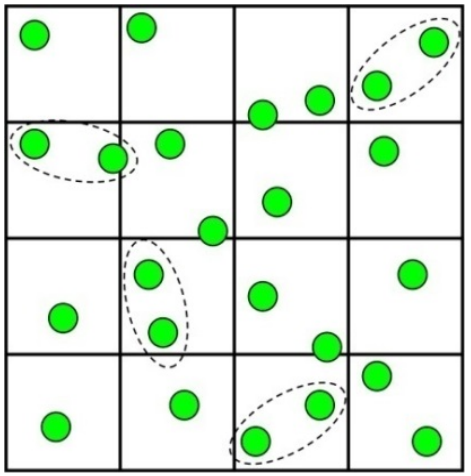

Not enough particles to capture physics

DSMC Convergence

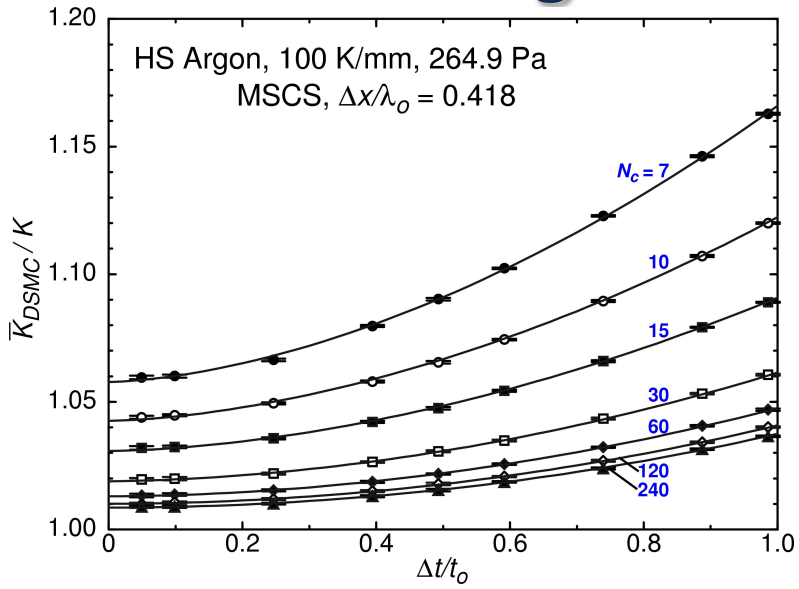

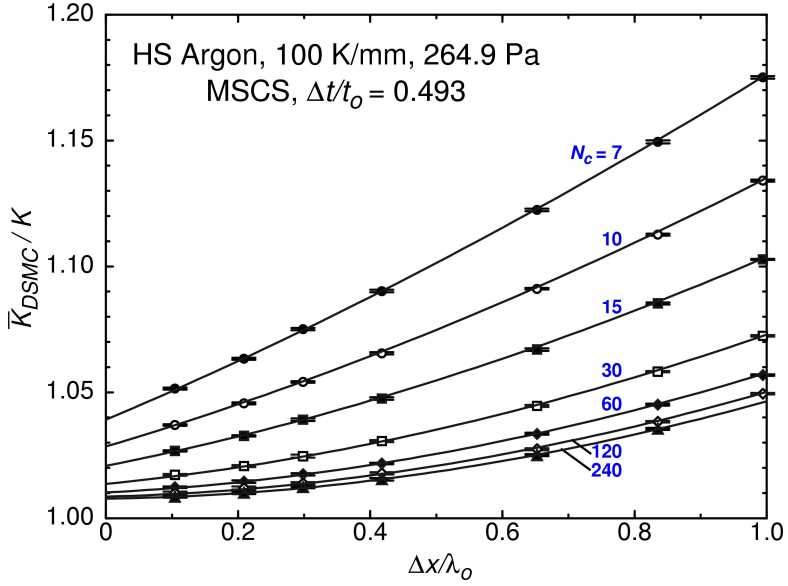

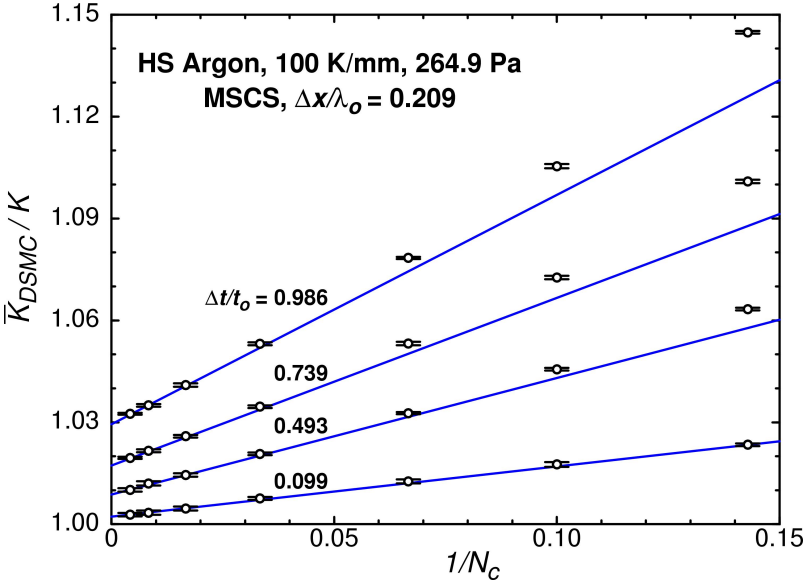

- Curves are best fits
- Error bars represent 95% confidence intervals
- Quadratic convergence for Δx, Δt
- First-order convergence $O(1/N_c)$, as $N_c \to \infty$
- Higher-order for long time steps
- For $N_c = 7$ and $\Delta t/t_o = 0.493$, convergence rate appears linear in $\Delta x/\lambda_o$

Functional Form of Error

Sandia National Laboratories

Functional form that represents DSMC data

- *Ad hoc* series expansion in Dx, Dt, and $1/N_c$
- Perform least-squares fitting of entire data set

$$\frac{K_{DSMC}}{K} = 1.0000 + 0.0286\Delta\tilde{t}^2 + 0.0411\Delta\tilde{x}^2 - 0.0016\Delta\tilde{x}^3 - 0.023\Delta\tilde{t}^2\Delta\tilde{x}^2 +$$
$$-\frac{0.111}{N_c} + \frac{1}{N_c}\left[1.22\Delta\tilde{x} - 0.26\Delta\tilde{x}^2 + 0.97\Delta\tilde{t}^{3/2} + \ldots\right] + 0.95\frac{\Delta\tilde{t}^2}{N_c^2} + \ldots$$

Cross terms show convergence behavior is complex

Rader D. J., Gallis M. A., Torczynski J. R., Wagner W., "DSMC Convergence Behavior of the Hard-Sphere-Gas Thermal Conductivity for Fourier Heat Flow", *Phys. Fluids*, 18, 077102, 2006.

DSMC Numerical Error

Sandia National Laboratories

Traditional DSMC rule-of-thumb guidelines:

- Take enough samples to drive statistical error down to "acceptable" level
- Keep time step smaller than ~1/4 mean collision time
- Keep cell size smaller than ~1/3 mean free path
- Use a minimum of ~20 particles per cell

These guidelines give 2% error, which is similar to the uncertainty in measured transport properties for most gases

- DSMC is subject to the same constraints as other numerical methods.
- DSMC is correct to the limit of vanishing discretization.

Infinite-Particle Convergence

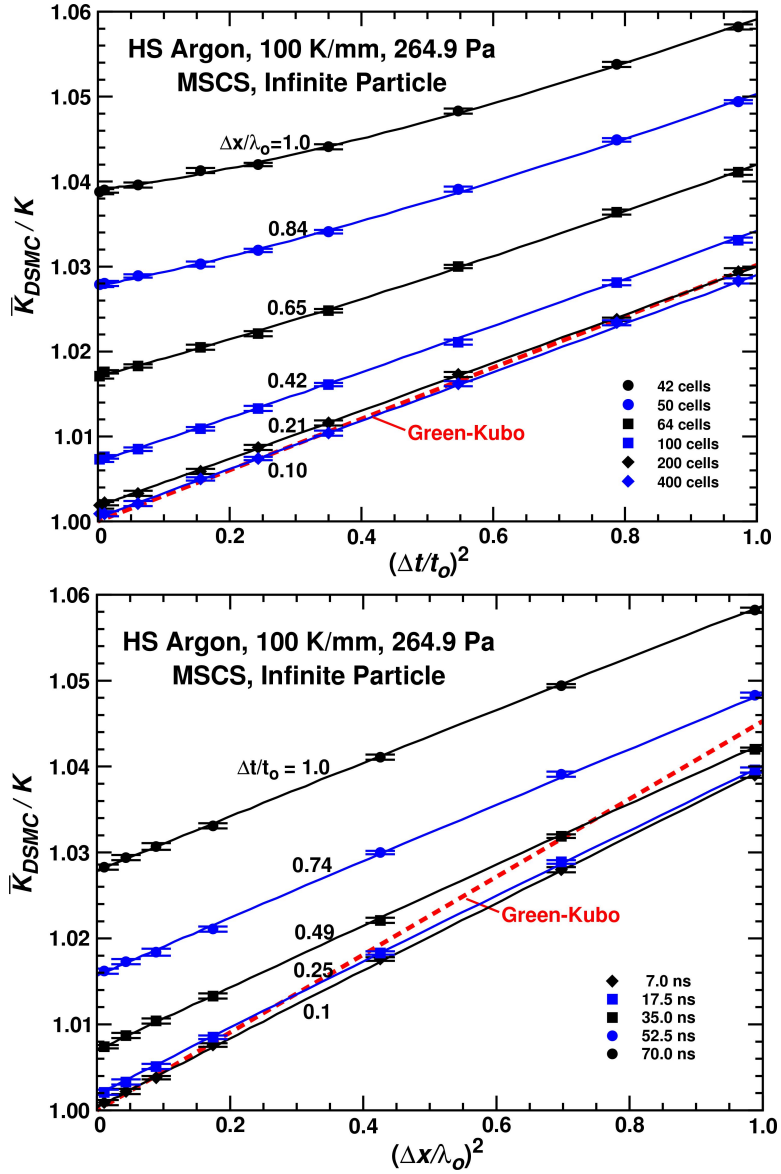

- Finite-particle error removed: values "extrapolated" to $N_c \rightarrow \infty$
- 63 extrapolated data points
- Error bars: fitting uncertainty
- Quadratic convergence in time step and cell size
- *Qualitative* agreement with *Green-Kubo* theory, but slopes are different
- Lines are best fits of data

Could the N-S Equations be extended ?

- Velocity-slip and Temperature jump

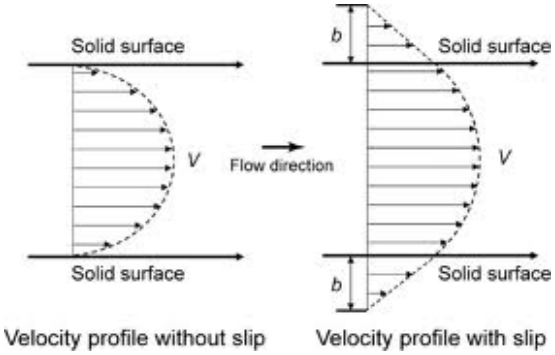

- Modified transport coefficients (viscosity, conductivity, diffusivity)

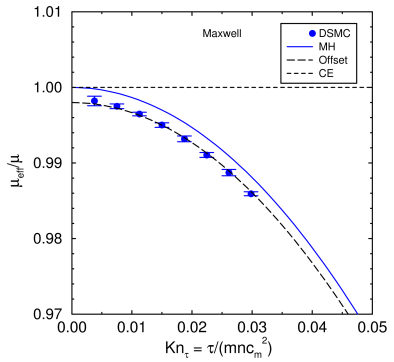

- Hybrid Schemes (NS-DSMC)

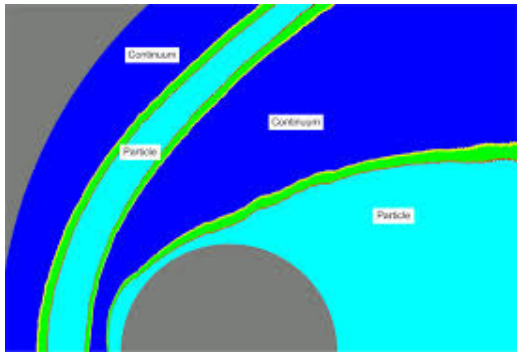

Gas Flow in a Microscale Tube

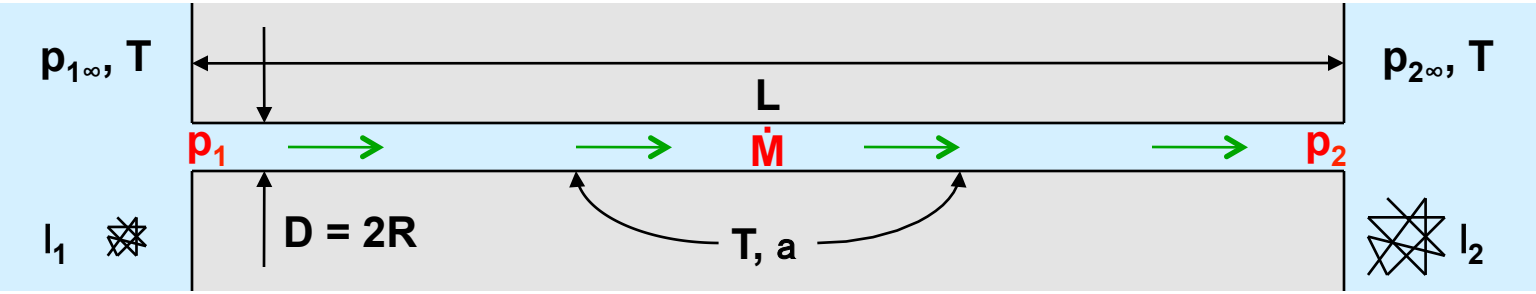

Investigate steady isothermal gas flow in microscale tube

- Tube is long and thin (L >> D) with circular cross section
- Tube joins gas reservoirs at different pressures ($p_{1\infty} \geq p_{2\infty}$)
- Tube and reservoirs have same temperature (T)
- Molecules partially accommodate ($a \leq 1$) when reflecting
- Flow speed << molecule speed, laminar, no turbulence

Determine the mass flow rate and the pressure profile

- General physics-based closed-form expressions
- Free-molecular to continuum (arbitrary mean free path l)
- Theory and molecular-gas-dynamics simulations

Extending the Navier-Stokes equations

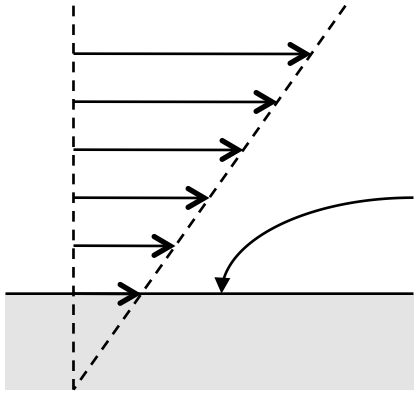

slip velocity

$$U_S - U_W = \frac{2-\alpha}{\alpha}\left\{\frac{\mathrm{Kn}}{1-b\mathrm{Kn}}\left(\frac{\partial U}{\partial n}\right)_S\right\}$$

- Mean free path at STP is 0.06 mm, large enough to matter
- Silicon channels of <10 μm height and >10 μm length

- Accurate mass flow rate needs accurate velocity profile
- Slip boundary condition improves prediction by Navier-Stokes equations

Boundary Conditions for Accurate Transport

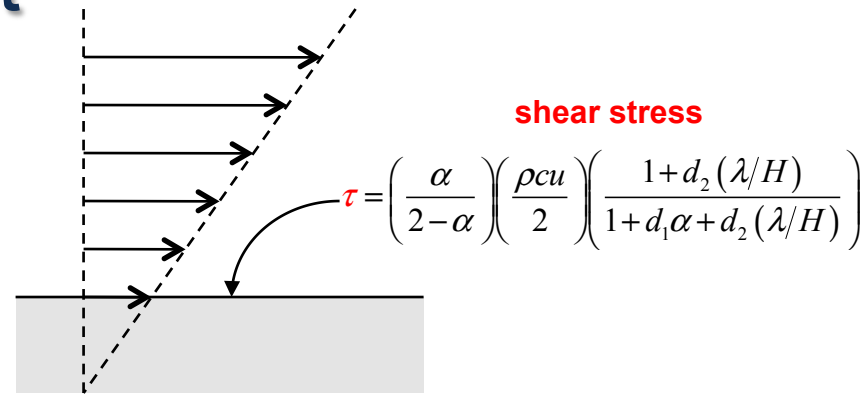

- Transport rates are of primary importance
  - Mass, momentum, energy
- Fields are of secondary importance
  - Concentration, velocity, temperature

Construct boundary conditions to give accurate transport

- When used with Navier-Stokes equations
- For free-molecular, transition, slip, continuum

Resulting fields are only qualitatively correct

- Fields are accurate in continuum limit

Mass Flow Rate Has Correct Limits

Sandia National Laboratories

Approximate Closed-Form Expression

$$\dot{M} = \dot{M}_C\left(1+\frac{8p_\lambda}{p_m}\varpi\left[p_1,p_2\right]\right),\quad \varpi\left[p_A,p_B\right]=\frac{2-\alpha}{\alpha}\left\{1+b_1\alpha+\left(\varepsilon b_0-1-b_1\alpha\right)\frac{b_2p_\lambda}{p_A-p_B}\ln\left[\frac{p_A+b_2p_\lambda}{p_B+b_2p_\lambda}\right]\right\}$$

Continuum

$$\dot{M}_C=\frac{D^4p_m\left(p_1-p_2\right)}{16\mu c^2L}$$

Slip

$$\dot{M}_S=\dot{M}_C\left(1+\frac{8p_\lambda}{p_m}\varpi_S\right),\quad \varpi_S=\frac{2-\alpha}{\alpha}\left(1+b_1\alpha\right)$$

Free-Molecular

$$\dot{M}_F=\dot{M}_C\left(\frac{8p_\lambda}{p_m}\varpi_F\right),\quad \varpi_F=\frac{2-\alpha}{\alpha}\varepsilon b_0$$

Continuum Orifice

$$\dot{M}_{OC}=\frac{R^3\rho_{m\infty}}{3\mu}\left(p_{1\infty}-p_{2\infty}\right)$$

Free-Molecular Orifice

$$\dot{M}_{OF}=\pi R^2\frac{mc}{4}\left(n_{1\infty}-n_{2\infty}\right)$$

Free-Molecular Short Tube

$$\dot{M}_{TF}=\dot{M}_{OF}\Big/\left(1+\left(\alpha L/D\right)\right),\quad \alpha L/D\ll 1$$

Expression reproduces known limits correctly

Continuum	Not affected by e, b_0, b_1, b_2
Slip	Determined by b_1
Free-Molecular	Determined by e, b_0
Orifice/Short-Tube	Determined by e, b_0

Ewart et al. (2006) Tube Experiments

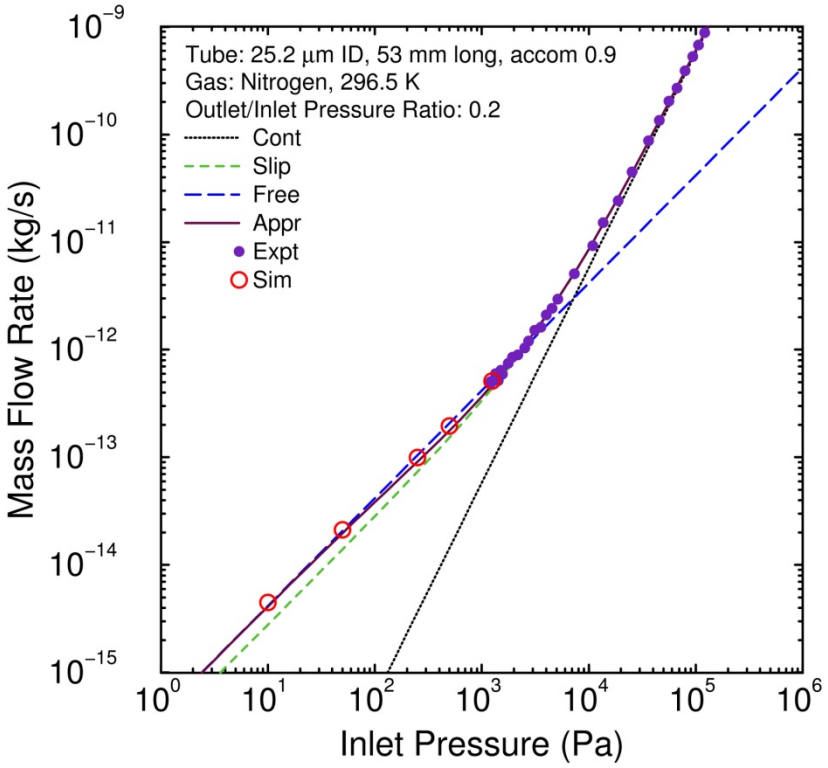

Tube Mass Flow Rate

$$\dot{M} = \dot{M}_C\left(1+\frac{8p_\lambda}{p_m}\varpi\left[p_1,p_2\right]\right),\quad \dot{M}_C = \frac{D^4}{16}\frac{p_m\left(p_1-p_2\right)}{\mu c^2 L}$$

$$\varpi\left[p_A,p_B\right] = \frac{2-\alpha}{\alpha}\left\{1+b_1\alpha+\left(\varepsilon b_0-1-b_1\alpha\right)\frac{b_2p_\lambda}{p_A-p_B}\ln\left[\frac{p_A+b_2p_\lambda}{p_B+b_2p_\lambda}\right]\right\}$$

$$\rho = \frac{mp}{k_BT},\ \mu=\mu[T],\ c=\sqrt{\frac{8k_BT}{\pi m}},\ \lambda=\frac{2\mu}{\rho c},\ p_\lambda=\frac{p\lambda}{D},\ p_m=\frac{p_1+p_2}{2},\ \mathrm{Kn}_m=\frac{p_\lambda}{p_m}$$

$$\frac{\alpha L}{D}>10^3,\ \varepsilon\to 1,\ p_1\to p_{1\infty},\ p_2\to p_{2\infty};\ b_0=\frac{16}{3\pi},\ b_1=0.15,\ b_2=\frac{0.7\alpha}{2-\alpha}$$

Same values of e, b_0, b_1, b_2 used for all circular tubes

Values are unchanged from previous cases (no adjusting)

Relative to diameter, this tube length is essentially infinite

Mass flow rate measured for silica microscale tube

- D = 25.2 mm, L = 53 mm, a = 0.9, N_2, T = 296.5 K, p_2/p_1 = 0.2

Expression and simulations agree well with experiment

- Lowest experiment pressure is above Knudsen minimum
- Highest simulation pressure reaches experiment

Ewart et al. (2007) Channel Experiments

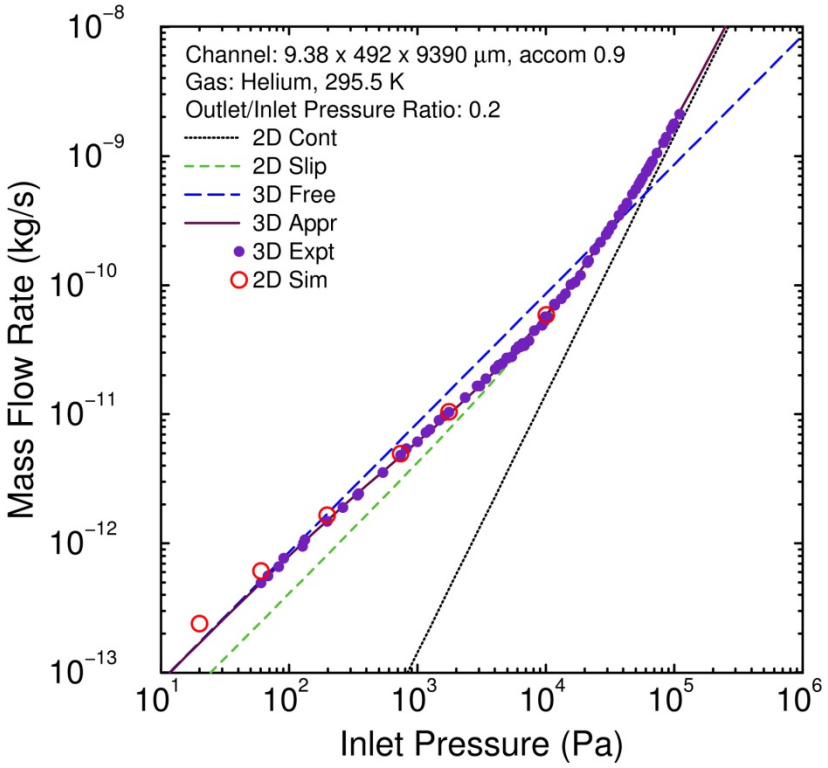

Channel Mass Flow Rate

$$\dot{M} = \dot{M}_C\left(1+\frac{6p_\lambda}{p_m}\varpi\left[p_1,p_2\right]\right),\quad \dot{M}_C = \frac{2WH^3}{3\pi}\frac{p_m\left(p_1-p_2\right)}{\mu c^2 L}$$

$$\varpi\left[p_A,p_B\right] = \frac{2-\alpha}{\alpha}\left\{1+b_1\alpha+\left(\varepsilon b_0-1-b_1\alpha\right)\frac{b_2p_\lambda}{p_A-p_B}\ln\left[\frac{p_A+b_2p_\lambda}{p_B+b_2p_\lambda}\right]\right\}$$

$$\rho = \frac{mp}{k_BT},\ \mu=\mu[T],\ c=\sqrt{\frac{8k_BT}{\pi m}},\ \lambda=\frac{2\mu}{\rho c},\ p_\lambda=\frac{p\lambda}{H},\ p_m=\frac{p_1+p_2}{2},\ \mathrm{Kn}_m=\frac{p_\lambda}{p_m}$$

$$b_0=3.28457,\ b_1=0.15,\ b_2=0.194,\ \varepsilon=0.725$$

Channel-flow expression correlates experiment values well

Derived for L×W×H rectangular channel just like for tube

b_0 from Kennard infinite-length free-molecular flow

b_1 = 0.15 as before to match slip regime for most gases

b_2 and e selected to match transition regime: L/W = 19.1

Mass flow rate measured for silicon microscale channel

- H,W,L = 9.38, 492, 9390 mm, a = 0.9, He, T = 295.5 K, p_2/p_1 = 0.2

Expression and simulations agree with experiment

- 2D simulation overpredicts 3D experiment at low pressures
- b_2 and e in channel expression are fit to experiment

Parallel-Plate Applications

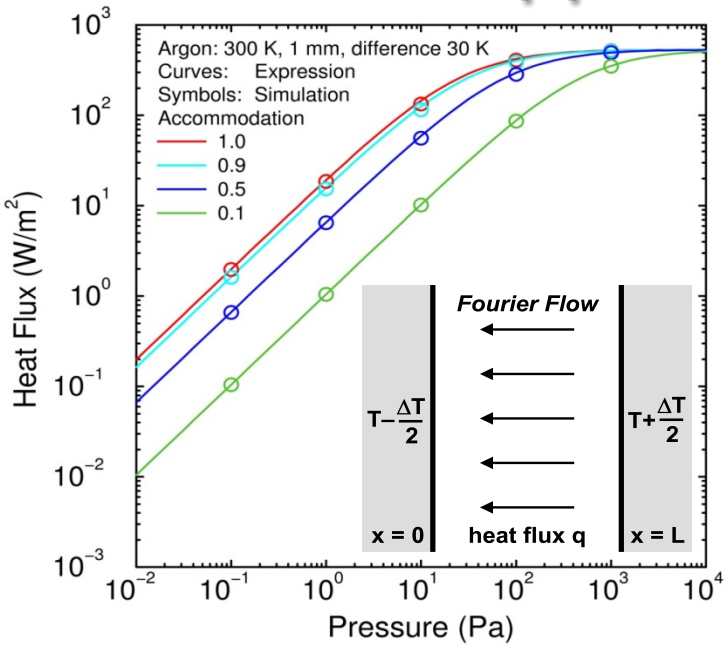

$$q = \frac{\alpha}{2-\alpha}\left(\frac{1+c_2(\lambda/L)}{1+c_1\alpha+c_2(\lambda/L)}\right)\left(1+\frac{\zeta}{4}\right)\frac{pc}{T}(T-T_w)$$

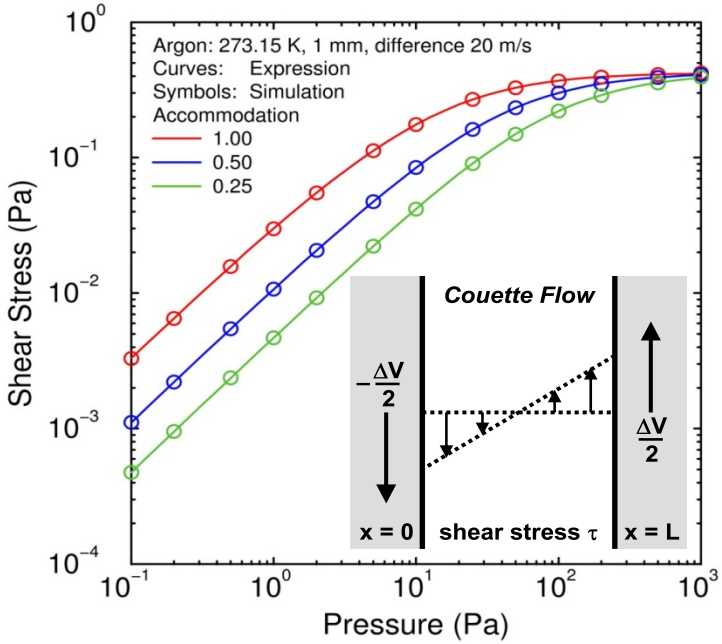

$$\tau = \frac{\alpha}{2-\alpha}\left(\frac{1+d_2(\lambda/L)}{1+d_1\alpha+d_2(\lambda/L)}\right)\frac{\rho c}{2}(u-u_w)$$

This philosophy works well for parallel-plate geometry

- Heat flux (Fourier flow): heat transfer
- Shear stress (Couette flow): momentum transfer

Accurate for free-molecular through continuum

- Low to high pressures, all accommodations

Parallel Efficiency: The Unfair Advantage

Sandia National Laboratories

- The advantages of DSMC come at a cost
- DSMC is computationally efficient but computationally intense
- Its successful application to real problems depends heavily on its parallel performance

- 1000x speedup required for some problems of interest
- Monte Carlo methods usually have good parallel performance
    - The workload depends mainly on the simulators within a cell
    - Relatively less need to communicate information between cells
    - Trivial to parallelize in velocity space

The necessary speedup can be achieved without any loss of accuracy or convergence characteristics through parallel computing

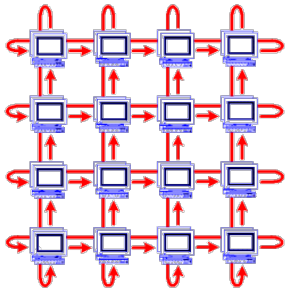

=

Top 5 Supercomputers (2014)

Sandia National Laboratories

Rank	Site	System	Cores	Rmax (TFlop/s)	Rpeak (TFlop/s)
1	National Super Computer Center in Guangzhou	**Tianhe-2 (MilkyWay-2)** - TH-IVB-FEP Cluster, Intel Xeon E5-2692 12C 2.200GHz, TH Express-2, Intel Xeon Phi 31S1P	3,120,000	33,862.7	54,902.4
2	DOE/SC/Oak Ridge National Laboratory	**Titan** - Cray XK7 , Opteron 6274 16C 2.200GHz, Cray Gemini interconnect, NVIDIA K20x	560,640	17,590.0	27,112.5
3	DOE/NNSA/LLNL	**Sequoia** - BlueGene/Q, Power BQC 16C 1.60 GHz, Custom	1,572,864	17,173.2	20,132.7
4	RIKEN Advanced Institute for Computational Science (AICS)	**K computer**, SPARC64 VIIIfx 2.0GHz, Tofu interconnect	705,024	10,510.0	11,280.4
5	DOE/SC/Argonne National Laboratory	**Mira** - BlueGene/Q, Power BQC 16C 1.60GHz, Custom	786,432	8,586.6	10,066.3

Programming for Next Generation and Exascale Machines

Sandia National Laboratories

- Millions of nodes likely
- Reduced memory per node
- Parallelism within node:
  - Multi-core: 16 and growing
  - Many-core: Intel Xeon Phi, 240 threads
  - GPUs: NVIDIA/AMD, 1000 warps
- Example:
  - LLNL BG/Q: 96K nodes, 16 cores/node + 4 MPI tasks/core

Programming model: MPI + X

- Goal is to decouple the science code from the hardware details

Necessary elements

- Adaptive gridding
- In-situ visualization
- Efficient communications
- Load balancing

Aiming for MPI+X via Kokkos

Sandia National Laboratories

- What is Kokkos:
  - Programming model in development at Sandia
  - C++ template library
  - Open-source
  - Stand-alone
- Goal: write application kernels only once, and run them efficiently on a wide variety of hardware platforms
- Two major components:
  - Data access abstraction via Kokkos arrays optimal layout & access pattern for each device: GPU, Xeon Phi, etc.
  - Parallel dispatch of small chunks of work auto-mapped onto back-end languages: CUDA, OpenMP, etc.

Developing an Exascale DSMC Code

Sandia National Laboratories

SPARTA = Stochastic PArallel Rarefied-gas Time-accurate Analyzer

General features

- 2D or 3D, serial or parallel
- Cartesian, hierarchical grid
  - Oct-tree (up to 16 levels in 64-bit cell ID)
  - Multilevel, general NxMxL instead of 2x2x2
- Triangulated surfaces cut/split the grid cells
  - 3D via Schwartzentruber algorithm
  - 2D via Weiler/Atherton algorithm
  - Formulated so can use as kernel in 3D algorithm
- C++, but really object-oriented C
  - Designed to be easy to extend
  - New collision/chemistry models, boundary conditions, etc.

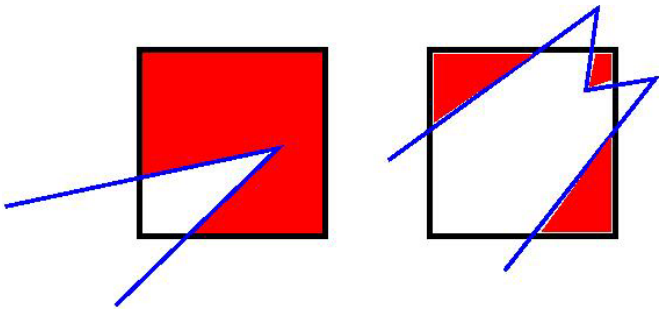

  - code available at http://sparta.sandia.gov

Adaptive Gridding

Sandia National Laboratories

- Create/adapt grid in situ, rather than pre-process & read in
- Examples: Generate around surface to user-specified resolution, adapt grid based on flow properties
- Algorithms should be efficient if they require only local communications

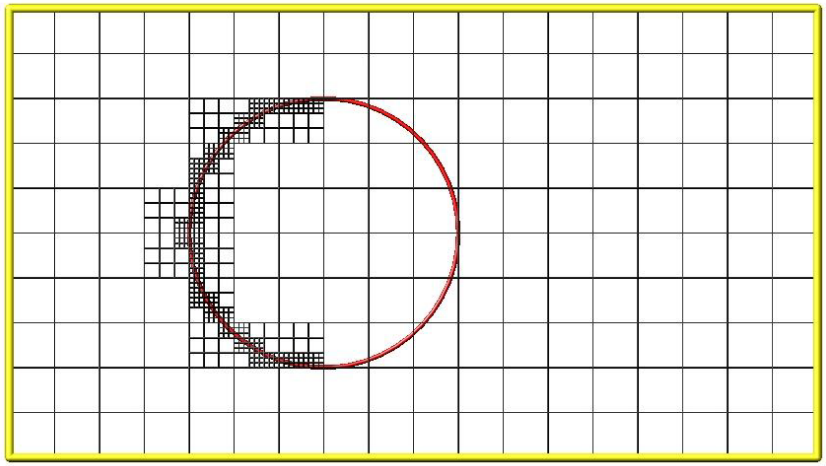

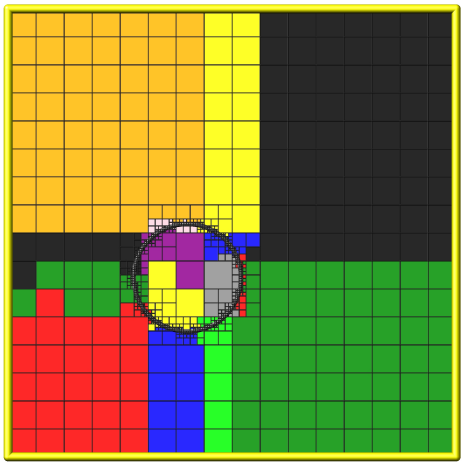

- Another setup task: label cells as outside/inside
- Simple if pre-processing, in situ easier for large problems

Simulation of Complicated Shapes

Sandia National Laboratories

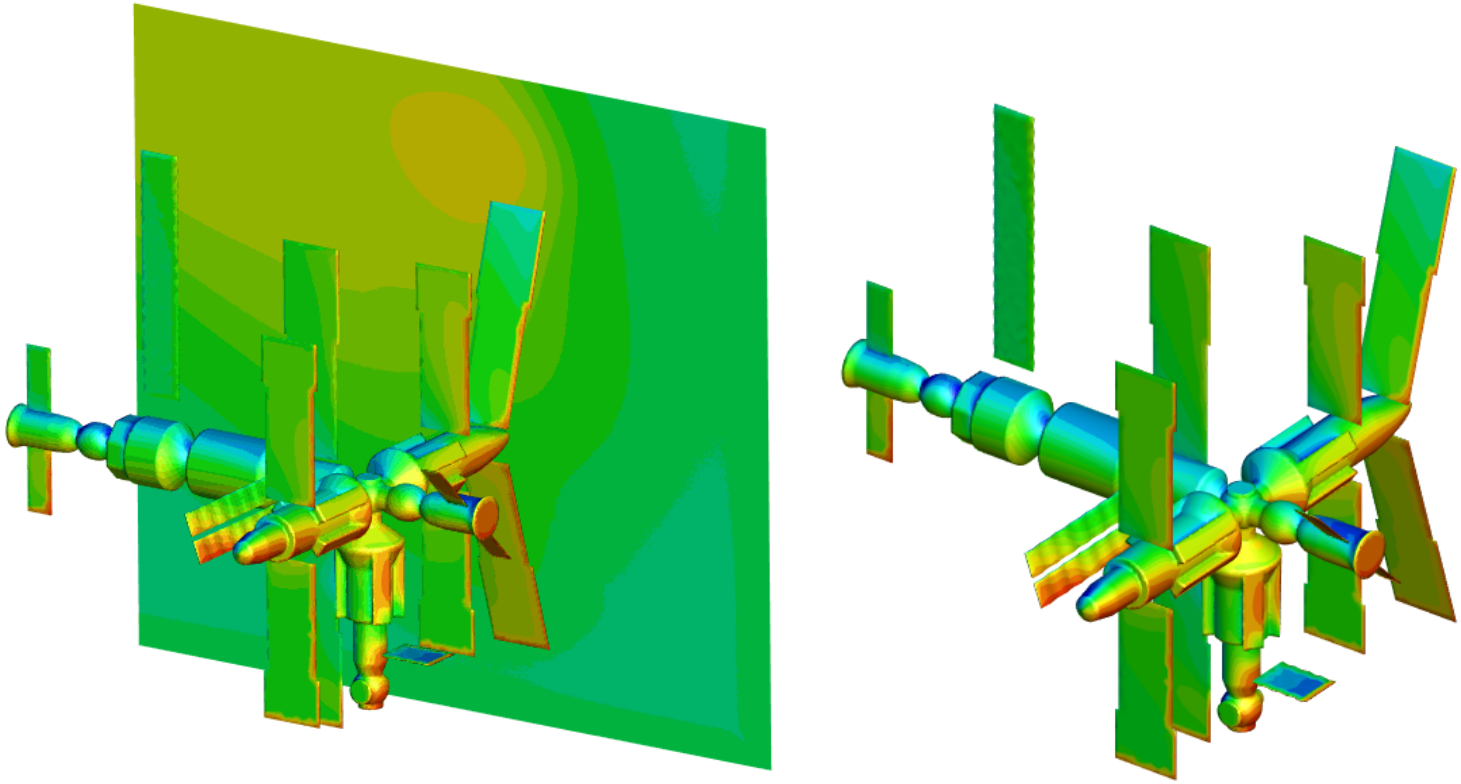

Grid generation (10^7 cells) completed in 0.3 seconds on 16 processors
Geometry comprises multiple “water-tight” bodies

In-Situ Visualization

Sandia National Laboratories

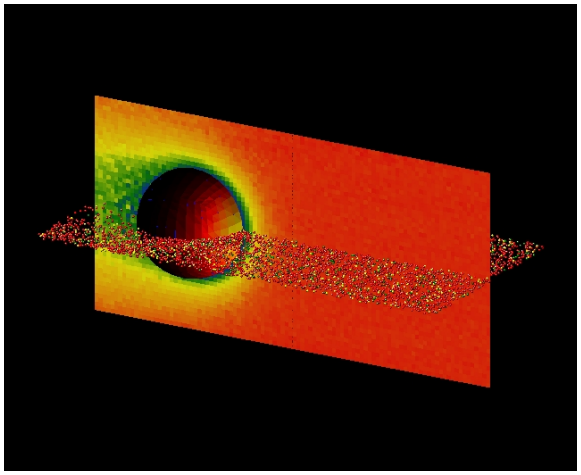

Not a replacement for interactive viz, but ...
Quite useful for debugging & quick analysis
At end of simulation (or during), instant movie

Render a JPG snapshot every N time steps:

- Each processor starts with blank image (1024x1024)
- Processor draws its cells/surfaces/molecules with depth-per-pixel
- Merge pairs of images, keep the pixel in front, recurse
- Draw is parallel, merge is logarithmic (like MPI Allreduce)

Images are ray-traced quality

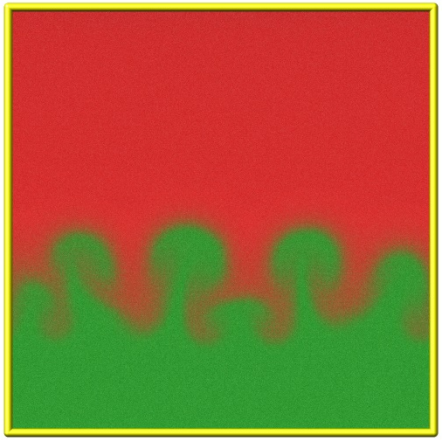

Load Balancing

Sandia National Laboratories

Balance across processors, static or dynamic
Granularity = grid cell with its molecules
Geometric method: recursive coordinate bisection (RCB)
Weighted by cell count or molecules or CPU

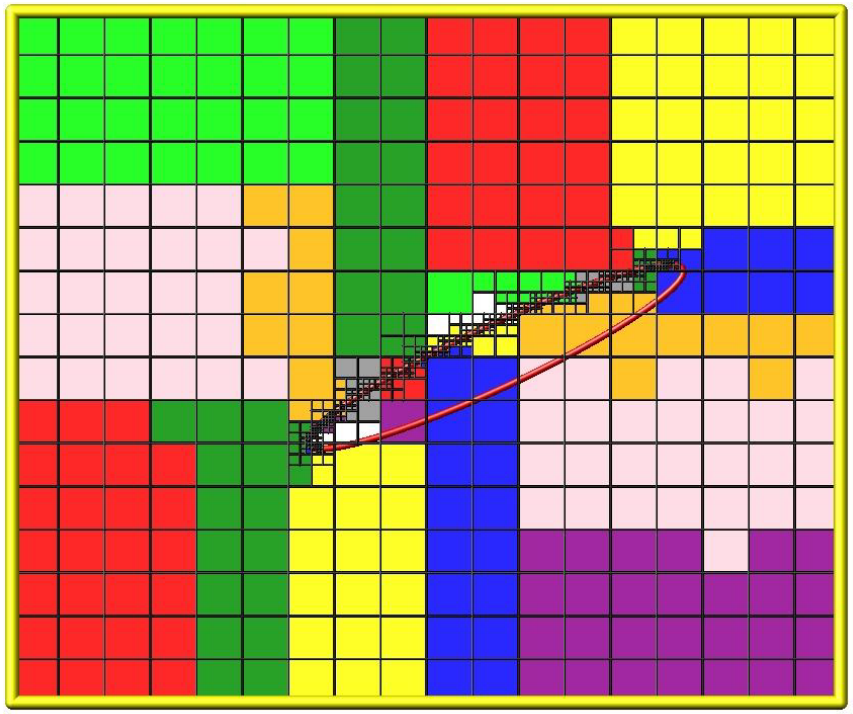

RCB is fast
Bigger cost is data move
Example:
1B cells on1024 BG/Q nodes
Worst case: move all cells
Balance time = 15 s:
(RCB=2, move=12, ghosts=1)

Efficient Communication

Sandia National Laboratories

- One processor = compact clump of cells via load balancing
  - Ghost region = nearby cells within user-defined cutoff
  - Store surface information for ghost cells to complete move

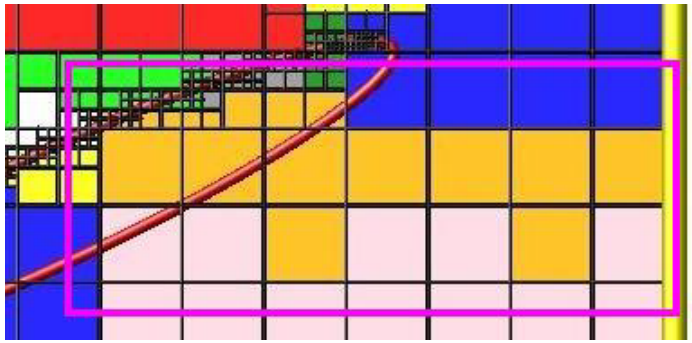

- Efficiently distributes grid information across processors
  - With sufficient cutoff, only one communication per step
  - Multiple passes if needed (or can bound molecule move)
- Communication with modest count of neighbor processors

SPARTA Benchmarking

Sandia National Laboratories

2 test cases:

- Free-molecular
  - Stress test for communication
  - 3D regular grid, 10^4-10^{11} (0.1 trillion) grid cells
  - 10 molecules/cell, 10^5-10^{12} (1 trillion) molecules
- Collisional
  - About 2x slower (sorting, collisions)
  - Same grid cell & molecule counts
- Effect of threading
  - 4 threads/core = 2x speed

SPARTA Benchmarking

Sandia National Laboratories

16 cores/node
1 task/core

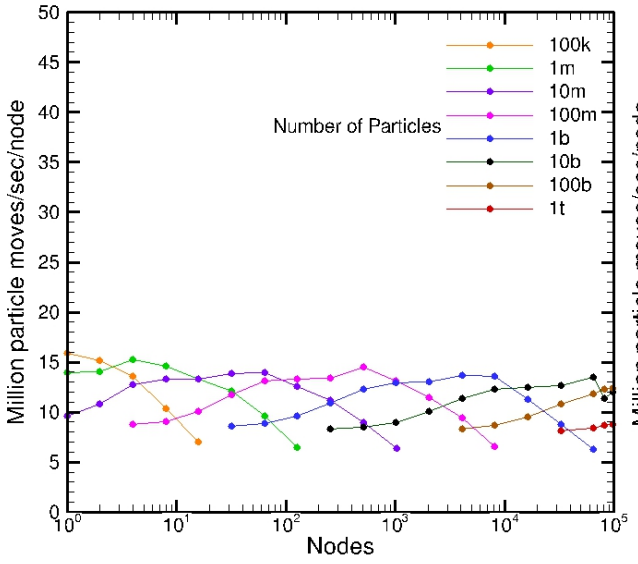

16 cores/node
2 tasks/core

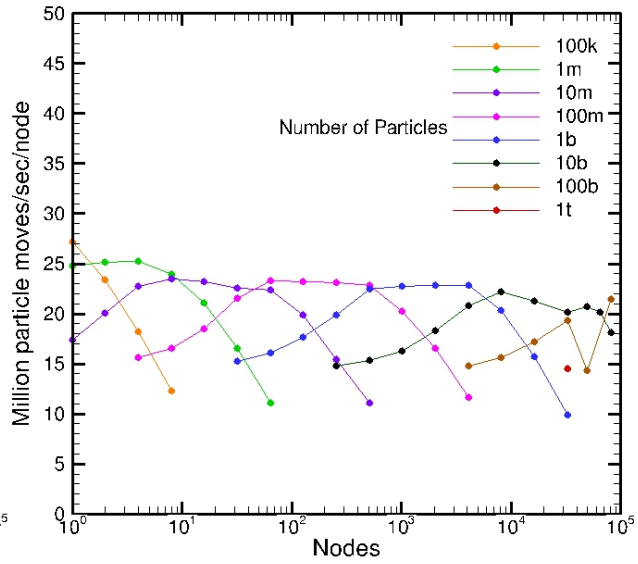

16 cores/node
4 tasks/core

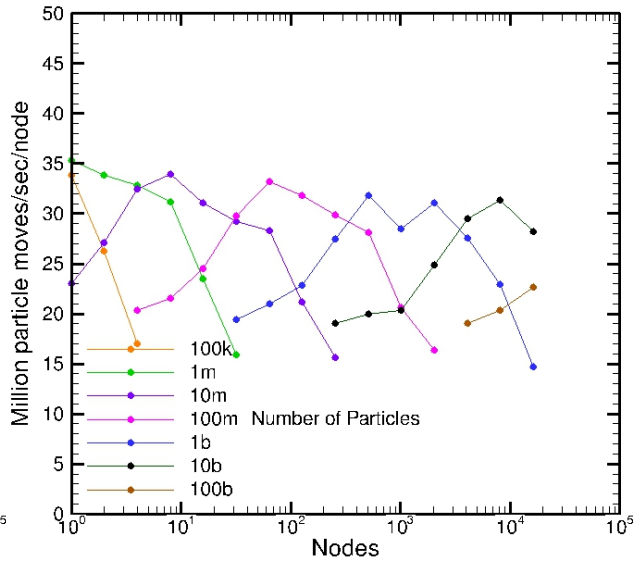

- Weak scaling indicates, 10% peak performance reduction from 1 to 10^6 cores
- 2 tasks/core gives 1.5x speedup, 4 tasks/core gives 2x speedup
- A total of 1 trillion simulators can be simulated on one third of the BG/Q
- Maximum number of tasks is 2.6 million

SPARTA Benchmarking (FM)

Sandia National Laboratories

16 cores/node, 1 task/core

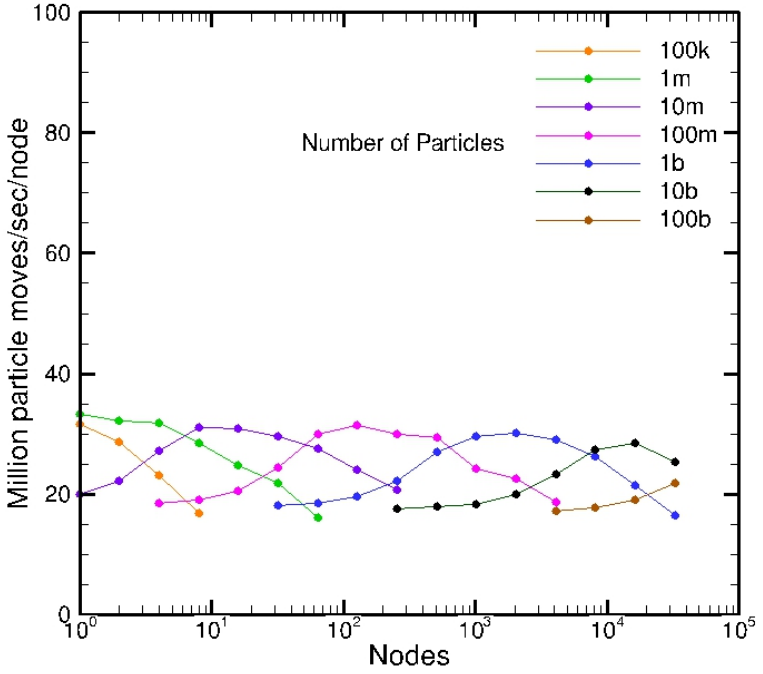

16 cores/node, 4 tasks/core

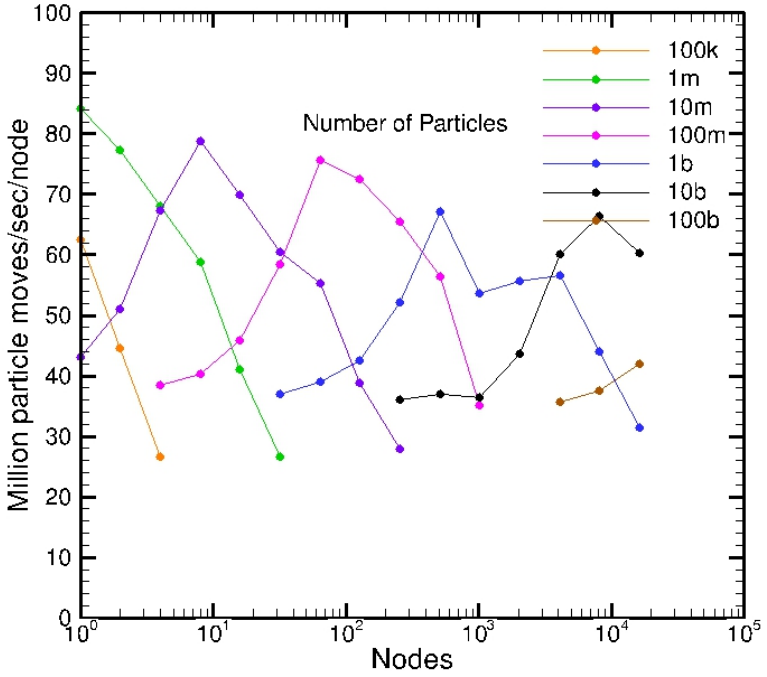

- Free-molecular (FM) calculations stress communications
- 2x speedup compared to collisional

Richtmyer-Meshkov Instability (RMI)

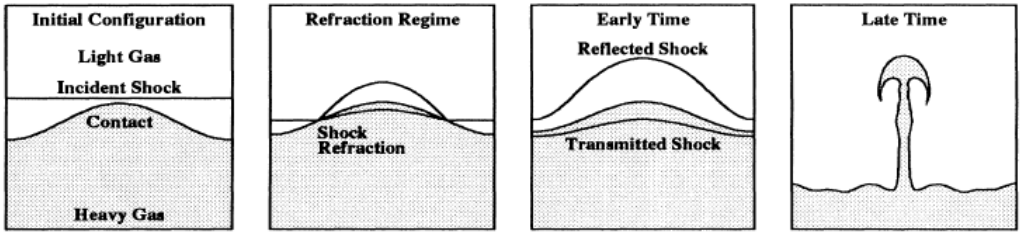

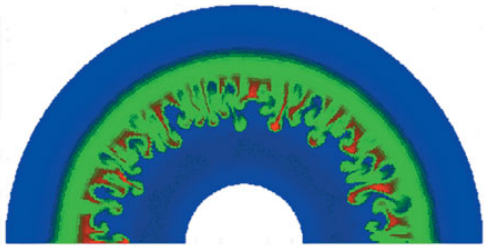

ICF target compression

Applications include Inertial Confinement Fusion (ICF), stellar evolution models, interaction of shocks with flames

RMI combines multiple compressible phenomena

- Shock interaction, refraction, reflection, transmission
- Hydrodynamic instability, including:
- Nonlinear growth
- Subsequent transition to turbulence
- Range of Mach numbers
- Chemical reactions (combustion)

RMI in He/Ar Mixture: Mach 1.2 Shock

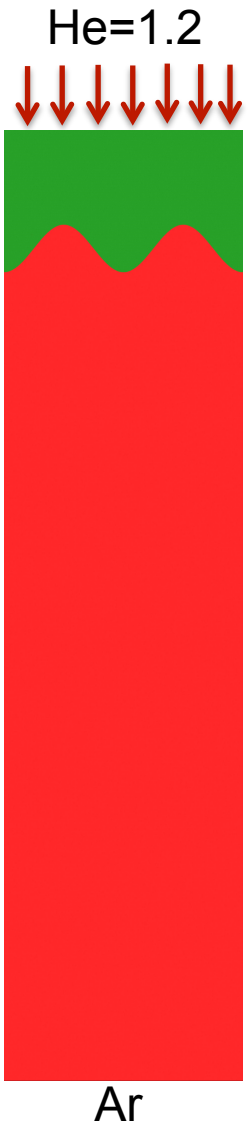

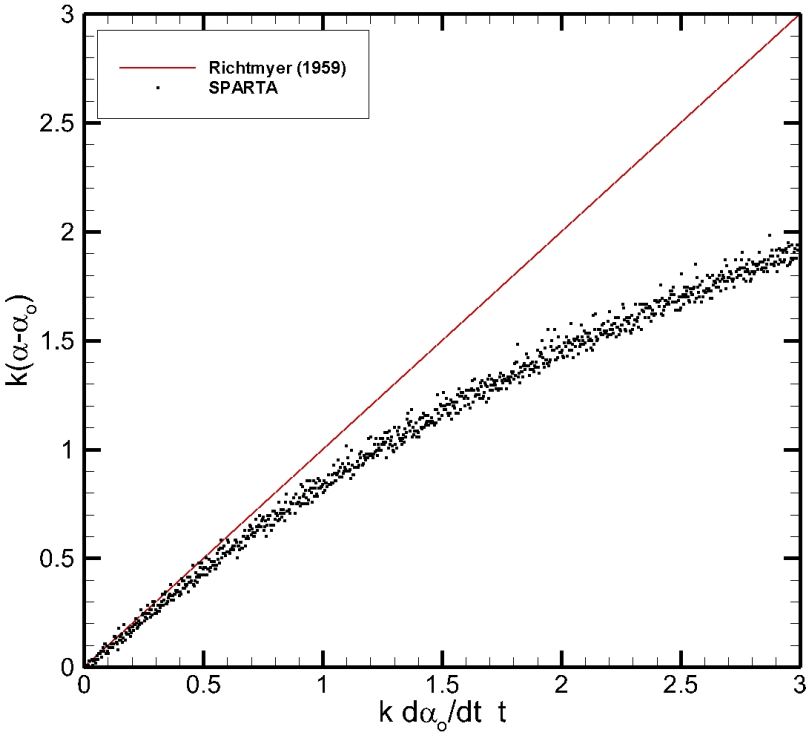

Non-dimensional amplitude for an initially small amplitude perturbation compared to Richtmyer's model for early time evolution

RMI in Air-SF_6 Mixture: Mach = 1.2 Shock

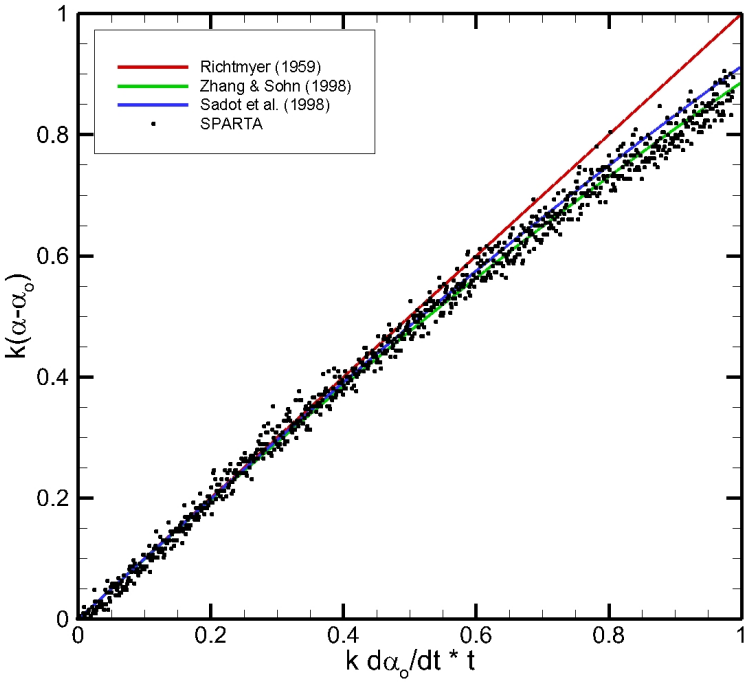

Non-dimensional amplitude for an initially small amplitude perturbation compared to theoretical/empirical models

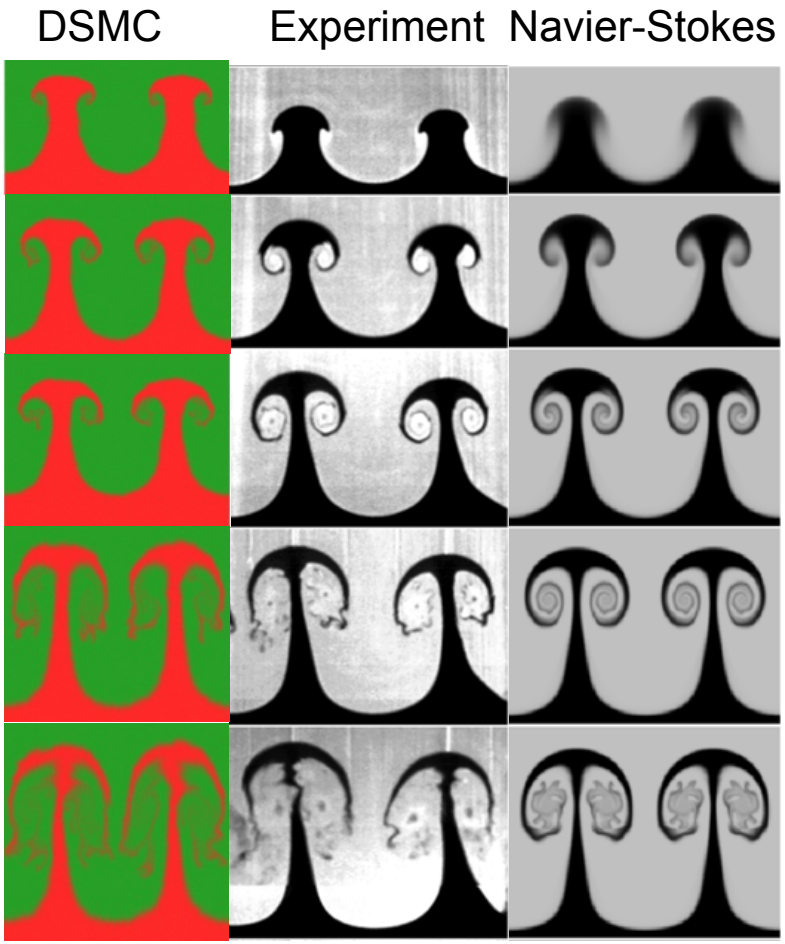

Conclusions

DSMC yields exquisite agreement with analytical results, where available

- Chapman-Enskog, Moment-Hierarchy theory
- Discretization & sampling errors understood

DSMC scales extremely well & can take full advantage of massively parallel platforms

- Can simulate unprecedented flow regimes
- Hydrodynamic instabilities, lower altitudes